Revised tuning of Ocean Drilling Program Site 964 and KC01B (Mediterranean) and implications for the $\delta^{18}O$, tephra, calcareous nannofossil, and geomagnetic reversal chronologies of the past 1.1 Myr

Lucas J. Lourens

Faculty of Geosciences, Department of Earth Sciences, Utrecht University, Utrecht, Netherlands

Received 5 December 2003; revised 12 May 2004; accepted 10 June 2004; published 4 September 2004.

[1] High-resolution color reflectance records of KC01 and KC01B (Calabrian Ridge, Ionian Sea) are presented and compared with a modified spliced high-resolution color reflectance record of Ocean Drilling Program (ODP) Site 964. This comparison revealed that KC01B is characterized by intensive deformation between ~27 and 28.5 m piston depth and that some sapropels are tectonically reduced in thickness. Moreover, the piston coring has caused considerable stretching in the top of KC01 and KC01B. Using a new splice of ODP Site 964 as guide, previous astronomical tuned timescales of KC01B and ODP Site 964 were evaluated. This evaluation resulted in a new sapropel-based astronomical timescale for the last 1.1 Myr. The new timescale implies a much more uniform change in sedimentation rate for the Ionian Sea cores. Two prominent excursions to lighter values in the $\delta^{18}O$ record of the planktonic foraminiferal species *Globigerinoides ruber* occur during marine isotopic stages 12 and 16 applying the new timescale. These shifts correspond with maxima in obliquity and are punctuated by minima in the precession cycle. They are absent in global ice volume records and are interpreted as reflecting a (summer) low-salinity surface water lens that floats on top of extremely saline intermediate and deep waters at times of the very low sea levels during these glacial periods. All biostratigraphic and magnetostratigraphic events found in KC01B and ODP Site 964 were re-dated according to the new timescale, and the ages of 33 tephra layers were reviewed. The new ages for the Calabrian Ridge 2 and 3 magnetic events in the Brunhes are concordant with minima in the global Sint800 composite record, derived from worldwide deep-sea records of relative paleointensity and have been attributed to the Big Lost and La Palma excursions, respectively. *INDEX TERMS:* 1520 Geomagnetism and Paleomagnetism: Magnetostratigraphy; 3344 Meteorology and Atmospheric Dynamics: Paleoclimatology; 4267 Oceanography: General: Paleoceanography; 4870 Oceanography: Biological and Chemical: Stable isotopes; 9604 Information Related to Geologic Time: Cenozoic; *KEYWORDS:* sapropel, tephra, Mediterranean, Pleistocene, magnetostratigraphy, biostratigraphy

Citation: Lourens, L. J. (2004), Revised tuning of Ocean Drilling Program Site 964 and KC01B (Mediterranean) and implications for the $\delta^{18}O$, tephra, calcareous nannofossil, and geomagnetic reversal chronologies of the past 1.1 Myr, *Paleoceanography*, *19*, PA3010, doi:10.1029/2003PA000997.

1. Introduction

[2] The astronomical timescale (ATS) for marine sequences in the Mediterranean was recently extended to ~13.5 Myr [*Hilgen et al.*, 2003]. This geological timescale is based on the calibration of sedimentary cycles such as sapropels (organic carbon-enriched layers), carbonate cycles, and diatomite layers to the computed time series of the quasiperiodic variations of Earth's orbit and axis [*Hilgen*, 1991a, 1991b; *Hilgen et al.*, 1995, 2000, 2003; *Hilgen and Krijgsman*, 1999; *Krijgsman et al.*, 1999; *Langereis et al.*, 1997; *Lourens et al.*, 1996a, 1996b, 1998]. The last ~1.1 Myr of the ATS was initially based on a detailed rock-magnetic and geochemical study of a 37 m long piston core (KC01B) from the Calabrian Ridge (Ionian Basin) [*Langereis et al.*, 1997]. This core was used to fill most of the gap between the oldest sapropel (S12) in piston core RC9-181 dated at 483 ka [*Lourens et al.*, 1996a] and the youngest sapropel (*v*) exposed in the land-based marine successions of the Vrica section dated at ~1.280 Ma [*Lourens et al.*, 1996b]. For tuning purposes, *Langereis et al.* [1997] used the actual sapropels as well as a number of "ghost-sapropels," inferred from specific geochemical and rock magnetic properties of the sediment. *Rossignol-Strick et al.* [1998] constructed concomitantly an independent age model through tuning the oxygen isotope record of KC01B to the ice sheet model of *Imbrie and Imbrie* [1980]. Differences between both age models are in the order of 0–5 kyr and result from the choice of two different target curves and hence the adopted time lags between insolation forcing and climate response [*Langereis et al.*, 1997] (see also *Hilgen et al.* [1993] and *Lourens et al.* [1996a] for discussion). Largest differences (in the order of 10 kyr) between both age models occur around 618 and 785 ka.

[3] In March 1995, Ocean Drilling Program (ODP) Site 964 was drilled close to KC01B with the main objective to construct an ATS [*Emeis et al.*, 2000]

0883-8305/04/2003PA000997$12.00

Table 1. Revised and Corrected Composite Depth Sections of ODP Site 964

Sakamoto et al. [1998]							This Study								
Hole	Core	Section	Centimeters	Meters Below Sea Floor	Revised Meters Composite Depth	SPLICE Interval	Hole	Core	Section	Centimeters	Meters Below Sea Floor	Revised Meters Composite Depth	Revised Composite Depth	Corrected Composite Depth	Δ, m
A	1	1	2	0.02	0.02	I	B	1	1	2	0.02	0.020	0.02	0.020	0.000
A	1	5	28	6.28	6.28		B	1	3	70	3.70	3.860	3.70	3.708	0.152
B	1	4	120	5.70	6.28	II	F	1	3	50	3.50	3.860	3.70	3.708	0.152
B	1	6	10	7.60	8.18		F	1	5	112	7.12	7.762	7.32	7.379	0.383
A	2	1	128	8.08	8.18	III	A	2	1	88	7.68	7.762	7.32	7.379	0.383
A	2	7	26	16.06	16.16		A	2	7	26	16.06	16.160	15.70	15.449	0.711
B	2	4	126	13.86	16.16	IV	B	2	4	126	13.86	16.160	15.70	15.449	0.711
B	2	7	36	17.46	19.76		B	2	6	150	17.10	19.384	18.94	18.648	0.736
A	3	2	120	19.00	19.76	V	A	3	2	84	18.64	19.384	18.94	18.648	0.736
A	3	6	130	25.10	25.86		A	3	7	26	25.56	26.300	25.86	25.303	0.997
E	3	4	106	20.56	25.86	VI	B	3	5	72	24.32	26.285	25.86	25.303	0.982
E	3	6	136	23.86	29.16		B	3	7	24	26.84	28.904	28.38	27.828	1.076
D	4	1	62	23.72	29.16	VII	D	4	1	38	23.48	28.904	28.38	27.828	1.076
D	4	6	134	31.94	37.38		D	4	6	102	31.62	37.057	36.52	35.834	1.223
B	4	3	72	30.82	37.38	VIII	A	4	5	64	32.44	37.060	36.52	35.834	1.226
B	4	6	130	35.90	42.46		A	4	7	66	35.46	39.900	39.54	38.690	1.210

independently from the nearby orbital tuned land-based marine sections of Singa and Vrica [*Hilgen*, 1991a; *Lourens et al.*, 1996a, 1996b]. A detailed comparison between ODP Site 964 and KCO1B is still lacking, which prevents a thorough evaluation of the proposed ATSs for the last 1.1 Myr. In this paper, high-resolution color reflectance records from KCO1B and KC01 are presented and compared with those obtained from ODP Site 964. This comparison will be used to evaluate the different age models for the Ionian Basin cores as well as deformation effects caused by drilling and soft-sediment faulting. On the basis of a uniform age-depth relationship, a new ATS for KCO1B, KC01, and ODP Site 964 is presented and its implications for (1) the oxygen isotope stratigraphy of the Mediterranean over the past 1.1 Myr, (2) magnetic reversals, (3) bio events, and (4) the Ionian Sea tephra chronology.

2. Materials and Methods

[4] Cores KC01 (25.93 m long) and KC01B (37.04 m long) were raised from a small ridge on the lower slope of the southern Calabrian Ridge (Pisano Plateau, 36°15.25′N, 17°44.34′E, 3643 m water depth) during cruise MD69 of the French R/V *Marion Dufresne* in June–July 1991. During ODP Leg 160 (March 1995), six holes were drilled at ODP Site 964 located at a water depth of 3650 m approximately 1 km NE from KC01 and KC01B. The studied sediments are fine-grained, nannofossil-rich, and contain distinct sapropels, tephra layers, and silt layers. All cores contain horizontally bedded successions with numerous faults.

[5] The color reflectance records from Holes 964A, 964B, 964D, 964E, and 964F were scanned with a hand-held Minolta CM 2002 spectrophotometer at 2 cm resolution on board the *JOIDES Resolution* just after the cores were opened [*Emeis et al.*, 1996]. The color reflectance records for KC01 and KC01B were scanned with a hand-held Minolta CM 503i spectrophotometer at 1 cm resolution and approximately 10 years (November–December 2001) after the cores were retrieved. In the passing years, KC01 and KC01B were stored at 5°C. This long storage time may have altered the fresh sediment colors, but the results of this study demonstrate that this effect is negligible and that characteristic color reflectance patterns can easily be identified. The color reflectance percentage at the 550 nm wavelength was selected to compare and correlate the cores in detail.

3. Results

3.1. Corrected Composite Depth of ODP Site 964

[6] During Leg 160, the initial meters below seafloor (mbsf) for each hole were transferred toward meters composite depth (mcd) by using color reflectance, gamma ray attenuation porosity evaluator (GRAPE), bulk density, and magnetic susceptibility [*Emeis et al.*, 1996]. However, the constructed depth sections were not corrected for possible disturbances resulting from coring operations, tectonic deformation, and/or differences in sedimentation rates. *Sakamoto et al.* [1998] presented revised composite depth (rmcd) sections that should have been corrected for most of these effects. First, a spliced record was constructed using a visual interhole correlation of the 2 cm resolution color reflectance data in combination with digitized core images. As much as possible, cores from a single hole were used as the basic "backbone" for the revised composite depth profile. Short sections from other holes were used to fill up gaps or areas of disturbed sediment within the "backbone" hole. The resulting rmcd scale of the spliced record has subsequently been used as target for the tuning of each individual hole through stretching and squeezing.

[7] Here I have chosen not to follow the same revised composite depth profile as proposed by *Sakamoto et al.* [1998] (Table 1). Some coring disturbances are present in the top of core 964A-1H, and I have considered the top of core 964B-1H to be more reliable. The most important difference between both spliced records is the choice of the second interval. *Sakamoto et al.* [1998] decided to use Hole B, which contains a "double" sapropel (SAP)

number 2. This sapropel can also be observed in Hole F but as a "single" layer. In both holes, some deformation features are present, and it is therefore not clear whether this sapropel has been tectonically reduced or doubled. The color reflectance records from KC01 and KC01B reflect, however, a "single" sapropel, and it seems therefore preferable to use Hole F instead of Hole B for the composite depth profile. For the sixth interval of the splice I refrained from using core 964E-3H because of some minor disturbances in section 5. The choice of Hole A instead of Hole B for the eighth interval of the splice is arbitrary and does not imply considerable change.

[8] A major consequence of using different holes for constructing the composite depth profile is that differences in sedimentation rates and coring operations between holes could lead to artificial stretching and squeezing. To visualize these effects, I have plotted the revised composite depth (rcd) value of characteristic points (tie points) in the composite color reflectance record against the mbsf value of their representative points in each hole and applied regression analysis on the data of the individual cores for all eight intervals of the splice (see electronic supplement)[1]. Disturbed intervals were excluded, which implies that in several of these cases, regression analysis was carried out on more than one undisturbed parts of the same core. From these analyses it appears that the slopes of the trend lines for the individual holes with respect to the splice could vary in the order of plus or minus 5–10% (5–10 cm for each meter rcd). Note that the hole used for a particular spliced interval has a slope of 1. These interhole relationships have been used to construct a new corrected composite depth (ccd) profile. For this purpose the average slope of all holes analyzed in each of the eight spliced intervals (including the slope of the hole used for the splice) was used to determine the average stretching factor for the hole used in the splice. Subsequently, all individual holes were plotted against the ccd profile using the new regression equations obtained from the relationships between mbsf and ccd of the tie points. A comparison between all holes plotted against ccd are given in the electronic supplement.

3.2. Color Reflectance Records of KC01 and KC01B

[9] Figures 1a and 1b show a comparison between the color reflectance records of KC01 and KC01B in meters piston depth (mpd) and the corrected composite depth profile for the top ~39 m of ODP Site 964. Sapropels, tephra layers, and silt layers are all marked by low color reflectance values and 33 tephra layers (Ionian, I1–I33) were detected in total. The late Pleistocene sapropels in KC01 and KC01B were labeled during the MD69 cruise [e.g., *Castradori*, 1993; *Sanvoisin et al.*, 1993] according to the sapropel codification of *Cita et al.* [1977]. The four distinct older sapropels of KC01B were labeled Sa-Sd after the cruise. In addition, two "ghost" sapropels were identified, termed S′ and S″ by *Langereis et al.* [1997]. Here this sapropel codification is maintained for comparison with the SAP code of ODP Site 964 [*Emeis et al.*, 1996, 2000].

[1]Auxiliary material is available at ftp://ftp.agu.org/apend/pa/2003PA000997.

[10] Detailed correlations between the color reflectance records of KC01, KC01B, and ODP Site 964 are not ambiguous for the topmost 2.5–3.5 m. The sedimentary successions of KC01 and KC01B are expanded with respect to the one of ODP Site 964, probably owing to strong suction of the piston during coring. Evidently, the top ~1.5 m at site KC01B has not been recovered, and almost all sediments of section 37 and top of section 36 have been sucked into section 38 (sections are indicated in Figures 1a and 1b). These coring problems are probably also responsible for extensive banding of the sediment in section 24 of KC01 and sections 35 and 36 of KC01B. The top of the banded interval contains a distinct dark tephra layer (I1) in KC01, whereas only some remains of this tephra are present in the disturbed interval of KC01B. The base of the banded interval is marked by a brownish colored well-layered turbidite. Both the turbidite layers as well as the tephra layer (although less pronounced) occur in Holes A, B, and D of ODP Site 964, indicating that the sediment succession of KC01 and KC01B is (almost) complete despite their coring deformation features. The top of KC01 includes the youngest, Holocene, sapropel S1 that can easily be correlated to Site 964.

[11] Five tephra layers (I2–I6) are present between I1 and S3 (Figures 1a and 1b) and were used as major tie points. A characteristic turbidite layer at ~3.6 ccd (m) in ODP Site 964 corresponds to a couple of thin silty layers in KC01 and KC01B. At ~8.75 mpd a second well-developed sapropel, labeled S3, has been recovered in KC01. This sapropel is markedly absent in ODP Site 964 and KC01B. However, both these cores reflect irregularities exactly at this level, indicating that the "missing" S3 [*Van Santvoort et al.*, 1997] has been tectonically reduced. The thin dark layer, termed "x" in ODP Site 964, most likely correlates with the thin layer just below the S3 in KC01. This thin layer is also present in KC01B (at 6.83 mpd) and has been interpreted by *Van Santvoort et al.* [1997] as being of volcanic origin.

[12] The site-to-site correlation of the interval between S3 and S5 is straightforward in case the sapropel S4 is interpreted as a "single" layer in ODP Site 964 (see section 3.1). Pronounced two-layered coarse-grained tephra layers are reflected by double peaks in the color reflectance records to low values between S3 and S4 (cf. I8) and between S4 and S5 (cf. I9). The S5 is rather thin in KC01B with respect to KC01 and ODP Site 964, which may indicate some tectonic reduction.

[13] The interval between S5 and S6 contains several thin silt and/or tephra layers that could be used for correlation between the cores. The interhole correlation is straightforward for the interval between S5 and I10, a distinct tephra layer found halfway between S5 and S6. A 15 cm thick turbidite is recovered approximately 50 cm below I10 in KC01B. This layer is absent in KC01 but recovered at ODP Site 964. Close inspection of KC01, however, reveals distorted sediments at 43 cm from the top of section 14 (~12.65 mpd) that could point to the existence of a fault. Detailed correlations between the cores indicate that approximately 0.6 m of sediment is missing in KC01 (see also section 3.3).

[14] The correlation of S6-S9 in KC01 and KC01B to SAP4-SAP7 in ODP Site 964 is unambiguous. This also

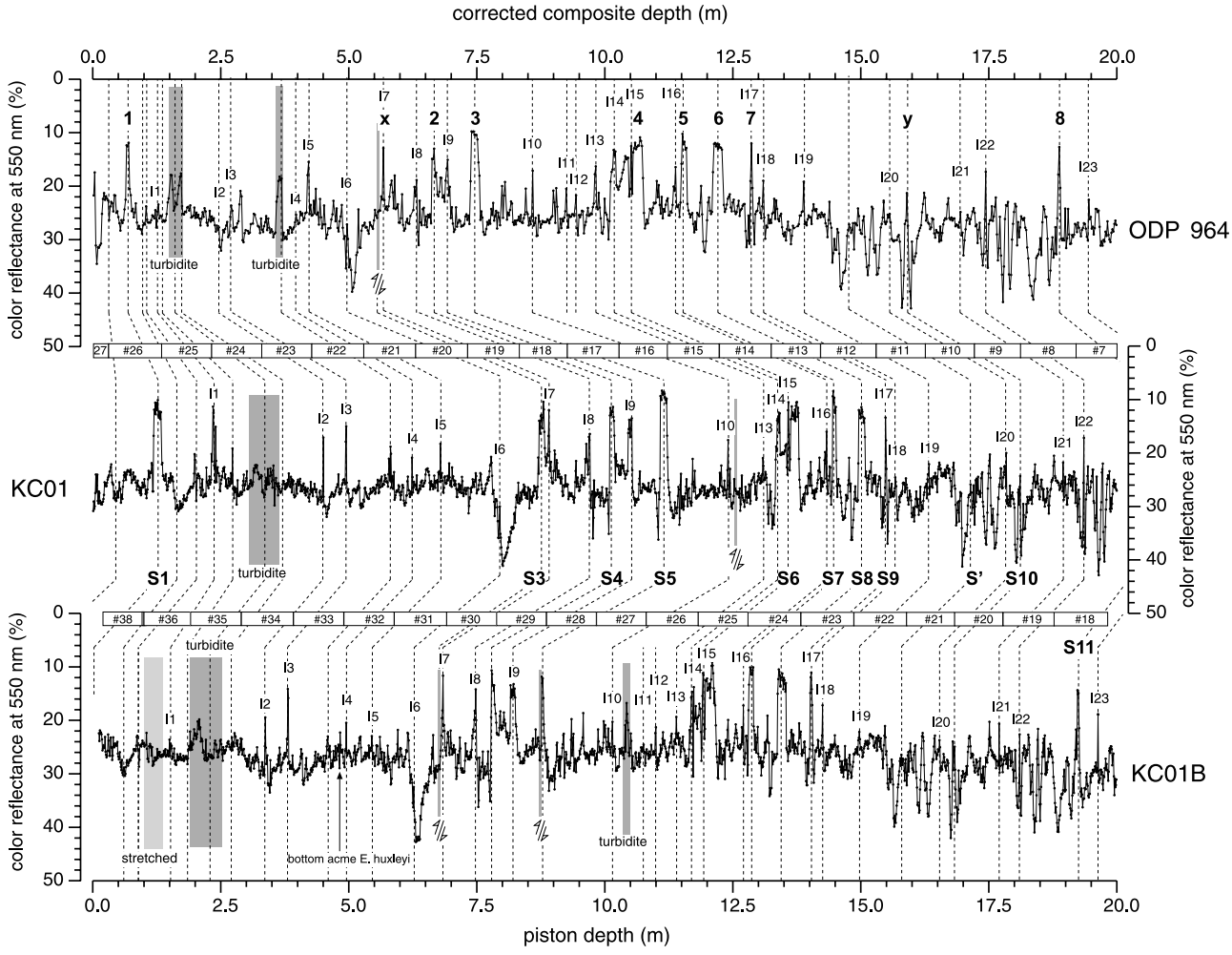

Figure 1a. Color reflectance at 550 nm (%) for cores KC01B, KC01, and ODP Site 964 against depth in meters. Sapropels for KC01 and KC01B are coded after amongst others *Langereis et al.* [1997], whereas the nomenclature for ODP Site 964 is after *Emeis et al.* [1996]. The numbers I1–I33 indicate Tephra layers.

holds for the correlation of S10-S12 and Sa-Sb in KC01 and KC01B to y SAP9 and SAP10-SAP12 in ODP Site 964, respectively. The "ghost" sapropel S′ [*Langereis et al.*, 1997; *Van Santvoort et al.*, 1997] is not reflected by a peak in the color reflectance records. A sapropel correlative to SAP11 in ODP Site 964 was not identified in KC01 and KC01B. However, *Langereis et al.* [1997] found peaks in Ba, NRM, and chi at the corresponding level that they interpreted as being the signature of a possible sapropel. Although this level is not characterized by very low color reflectance values, I have labeled this "ghost" sapropel as S*. Fifteen tephra layers were identified in the interval between S6 and Sb and one just below Sb.

[15] Three almost horizontally dipping faults occur at 24.93, 25.22, and 25.50 mpd in KC01B and may have caused some minor sediment loss with respect to ODP Site 964. The sediment at these levels is dark and coarse-grained, which could point to turbidite flows. The color reflectance patterns of the interval between 27 and 28.5 mpd in KC01B cannot be recognized in ODP Site 964. Close inspection of KC01B revealed four major faults of which three having a low angle (section 10, 40 and 56 cm from top; section 9, 27 cm from top) and one a high angle (section 10, 95 cm to section 9, 5 cm from top). A remarkable characteristic of this interval is the three-fold repetition of the color reflectance values toward high values (i.e., carbonate-rich sediment). The values and patterns resemble those found between 28.5 and 29.5 mpd in KC01B and between 29 and 29.5 ccd in ODP 964. I have interpreted this pattern repetition to result from soft-sediment slumping, causing the carbonate-rich layer to have repeated itself three times. Therefore it is not surprising that intensive deformation is found within the equivalent interval in Holes A and B of ODP Site 964. However, Hole D, which is used for the spliced record is not affected by tectonic deformation. This observation is strengthened by cross-checking with ODP Site 969 (Mediterranean Ridge, ~100 km south of Crete, Greece), which revealed almost the same characteristic color pattern as in ODP Site 964 Hole D [*Sakamoto et al.*, 1998; *Emeis et al.*, 2000].

[16] The correlation between KC01B and ODP Site 964 is straightforward below the disturbed interval. Sapropels S″,

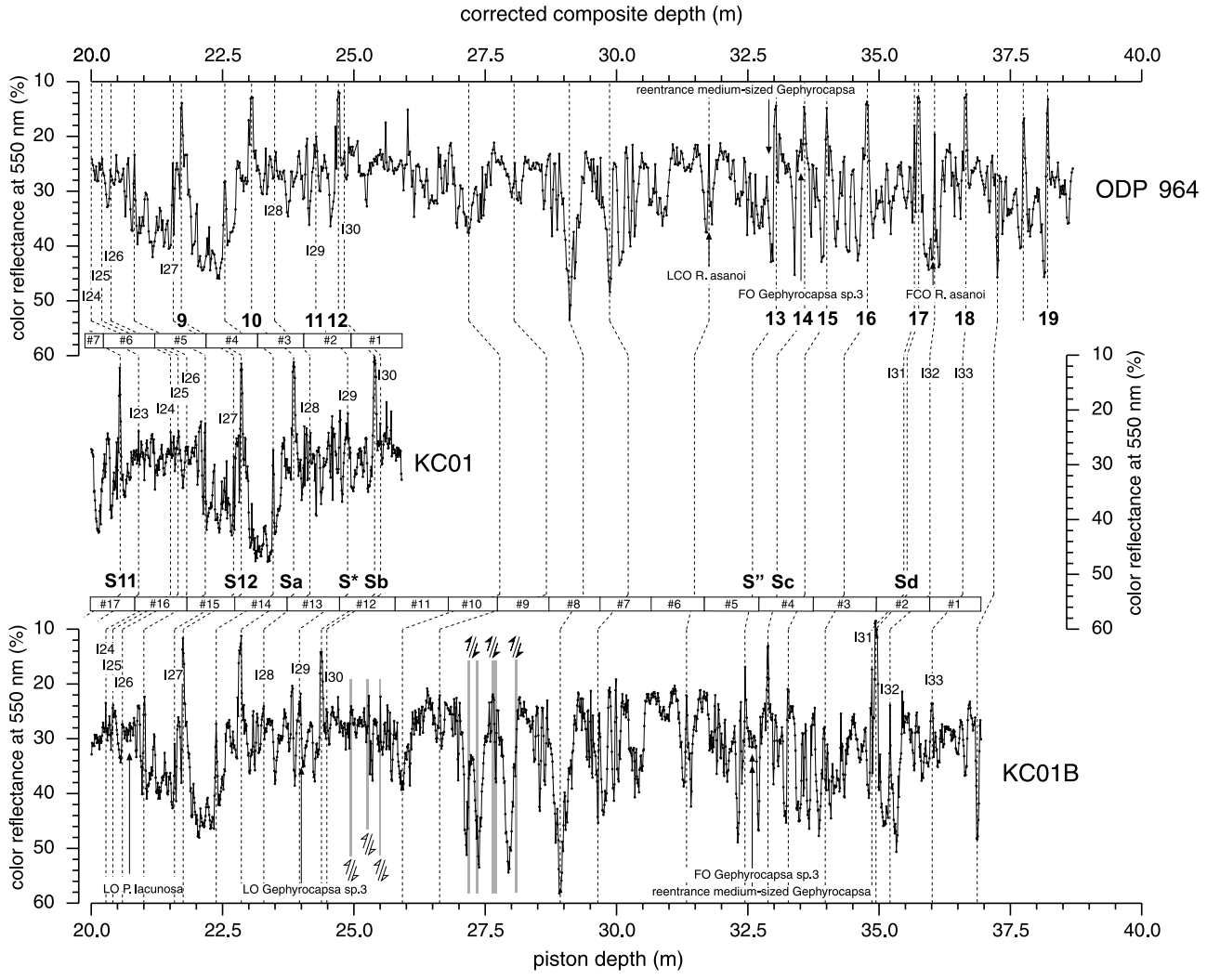

Figure 1b. Color reflectance at 550 nm (%) for cores KC01B, KC01, and ODP Site 964 against depth in meters. Sapropels for KC01 and KC01B are coded after amongst others *Langereis et al.* [1997], whereas the nomenclature for ODP Site 964 is after *Emeis et al.* [1996]. The numbers I1–I33 indicate Tephra layers in the depth interval between 20 m and 40 m.

Sc, and Sd unambiguously correlate with SAP13, SAP14, and SAP17. This correlation is confirmed by the identification of two distinct tephra layers just above (I31) and below (I32) Sd/SAP17. SAP16 of ODP Site 964 is not clearly marked in the color reflectance record of KC01B. In spite, a thin (~3 mm) sharp gray layer is present at the corresponding level (section 3, 26 cm from top) in KC01B, indicating that this sapropel has been tectonically reduced. The very bottom of KC01B is marked by extensive sediment banding and stretching with respect to ODP Site 964, probably owing to disturbance when the piston core was released from the surrounding sediments.

3.3. Depth Relationships Between KC01, KC01B, and ODP Site 964

[17] Figure 2a shows a XY plot of the mpd values of the tie points between KC01 and KC01B. The depth relation between KC01 and KC01B can be best described by one linear equation and two second-order polynomials for the top ~2 to ~10 mpd. These relationships are most likely not caused by differences in sedimentation rates but are probably due to coring operations (i.e., strength of the piston and penetration velocity). The break between the first two equations is related to the thick turbidite layer, whereas the second break is caused by the missing sapropel S3 in KC01B at ~6.82 mpd and is estimated to be ~25 cm. This value exceeds the thickness of the S3 (~12 cm) in KC01.

[18] From ~13 to 26 mpd the relationship between KC01 and KC01B can be described by a linear fit, which shows that the sediments in KC01B have been stretched in the order of 5% relative to KC01. This stretching is most likely due to coring operations but in theory can also be explained by slightly higher sedimentation rates in KC01B. The break between this linear equation and the second second-order polynomial coincides with sediment deformation in KC01 and the turbidite bed between S5 and S6 in KC01B. From

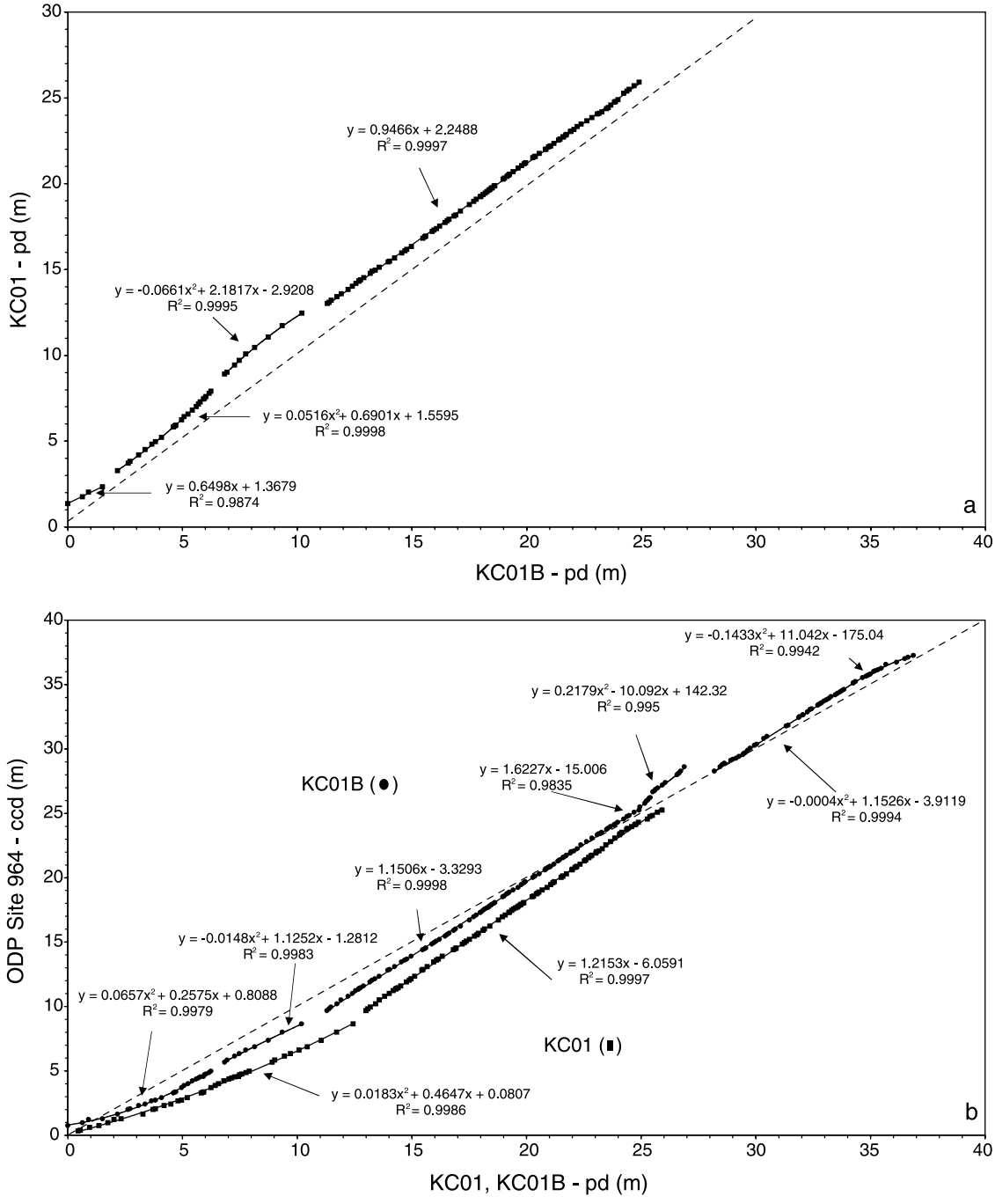

Figure 2. Depth comparison between KC01B, KC01, and ODP Site 964.

the equations it is evident that ~60 cm is missing in KC01 relative to KC01B.

[19] Similar kinds of relationships are obtained from the comparison of the mpd and ccd values of the tie points between KC01 and KC01B and ODP Site 964 for the top 25 m (Figure 2b). Evidently, the top 12–13 m of KC01 and KC01B are stretched with respect to ODP Site 964, whereas the intervals between 12–13 and 25–26 mpd in KC01 and KC01B are compressed with respectively ~20% and ~15% relative to ODP Site 964. The absence of a distinct S3 in ODP Site 964 would reveal that part of the sedimentary succession is missing at that site. Such a gap, however, is not evidenced by the depth relationships between ODP Site 964 and KC01, which may point to redeposition of sediments.

[20] Three second-order polynomials and one linear fit equation are needed to describe the relationship between ODP Site 964 and the bottom 12 m of KC01B. The tectonically disturbed intervals around 25 and 27.5 mpd and the stretched and banded interval at the bottom of KC01B are responsible for these breaks. In the electronic supplement I have included depth plots for the color

Table 2. Sapropel Chronology[a]

KC01B[b]				ODP 964[c]				KC01		This Study			
Level,[d] m	Sapropel	Si Cycle	Age_1, kyr	Level,[d] ccd	Sapropel	i Cycle	Age_2, kyr	Level,[d] m	Sapropel	i Cycle	Age_{new}, kyr	Δ_{new-1}, kyr	Δ_{new-2}, kyr
0.000	top		8	0.000	top		0	0.000	top	1	10.72/0/0.99[e]	2.72	0.0
	S1?	Si2		0.691	SAP 1	2	8	1.280	S1	2	8.5		0.5
	S3?	Si8	81				81	8.800	S3	8	81	0.0	0.0
6.840	X, below S3			5.675	X	8		8.930	X-below S3		82.84[g]		
7.805	S4	Si10	102	6.674	SAP 2	10	102	10.210	S4	10	101	−1.0	−1.0
8.780	S5	Si12	124	7.470	SAP 3	12	124	11.190	S5	12	124	0.0	0.0
11.950	S6	Si16	172	10.470	SAP 4	16	172	13.608	S6	16	172	0.0	0.0
12.873	S7	Si18	195	11.553	SAP 5	18	195	14.480	S7	18	195	0.0	0.0
13.460	S8	Si20	217	12.218	SAP 6	20	217	15.020	S8	20	216	−1.0	−1.0
14.046	S9	Si22	240	12.868	SAP 7	22	240	15.485	S9	22	239	−1.0	−1.0
15.740	S′	si26	288	14.794	Y			17.145	S′	26	288	0.0	
16.833	S10	Si30	331	15.903	Z			18.095	S10	30	331	0.0	
19.265	S11	Si38	407	18.860	SAP 8	38	407	20.535	S11	38	407	0.0	0.0
21.715	S12	Si44	461	21.735	SAP 9	44	461	22.855	S12	48	502	41.0	41.0
22.850	Sa	Si50	529	23.043	SAP 10	46	483	23.850	Sa	52	553	24.0	70.0
24.005	S*	si54	575	24.283	SAP 11	54	575	24.895	S[d]	56	596	21.0	21.0
24.390	Sb	Si56	597	24.702	SAP 12	56	597	25.395	Sb	58	618	21.0	21.0
25.025	*	si58	618	25.600						60	647	29.0	
28.870	*	si74	785	29.030						74	784	−1.0	
30.440	*	si82	862	30.800						82	861	−1.0	
	*	si86	908[f]										
32.455	S″	si90	955	33.060	SAP 13	90	955			90	954	−1.0	−1.0
32.895	Sc	Si92	976	33.577	SAP 14	92	977			92	976	0.0	−1.0
33.315	*	si94	997	34.009	SAP 15	94	997			94	997	0.0	0.0
33.970	*	si96	1027	34.767	SAP 16	96	1027			96	1026	−1.0	−1.0
	*	si98	1048[f]										
34.933	Sd	Si100	1070	35.725	SAP 17	100	1070			100	1069	−1.0	−1.0
	*	si102	1091[f]										
36.000	*	si104	1111	36.656	SAP 18	102	1091			104	1111	0.0	20.0
	*	si108	1144[f]										
36.950	base										1143[h]		
				38.212	SAP 19	104	1111			112	1185		74.0

[a]Age calibration points are based on revised sapropel midpoints (m) and refer to the ages of their correlative 3 kyr lagged insolation maxima.
[b]From *Langereis et al.* [1997].
[c]From *Emeis et al.* [2000].
[d]Levels in meters refer to the modified piston depths of KC01B and corrected composite depth of ODP 964 as used in this study.
[e]Age of the top of KC01B, ODP 964, and KC01 based on color correlation to ODP Site 964.
[f]Levels were excluded as calibration points.
[g]Age of the tephra layer X just below the S3 obtained from linear interpolation between the S3 and S4 of KC01.
[h]Age of the base of KC01B based on color correlation to ODP 964.

reflectance records of KC01 and KC01B transferred to the ODP Site 964 ccd values by using the relationships of Figure 2b. Following this procedure, the sediment repetition in KC01B has been eliminated.

4. Discussion

4.1. Sapropel Chronology

[21] The construction of a sapropel-based astronomical timescale for the Mediterranean late Neogene has started with the pioneering work of *Rossignol-Strick* [1983, 1985], who attributed sapropel formation to African monsoons as an immediate response to orbital insolation. Rossignol-Strick constructed a monsoon index based on the precession-dominated summer insolation gradient between the Tropic of Cancer and the Equator. The basis for her monsoon index is the astronomical calculation of *Vernekar* [1972], and she applied this orbital chronology to determine the ages of the sapropels. Following her pioneering work, *Hilgen* [1991a] in addition showed that small- and large-scale groups of sapropels correlate with maximum values in the 100 and 400 kyr cycles of eccentricity. He used the late Pleistocene phase relationships to construct an astronomical timescale for the sapropels and sapropel groups of late Pliocene to early Pleistocene age. On the basis of radiocarbon dating of the youngest sapropel (S1), *Hilgen* [1991a] furthermore proposed a 4 kyr time lag between the midpoints of each individual sapropel and their correlative precession minimum. This assumption in combination with the use of the precession index derived from astronomical solution Ber90 [*Laskar*, 1988; *Berger and Loutre*, 1990] resulted in a slightly modified timescale for S1–S12. Discrepancies between the insolation ages of *Rossignol-Strick* [1983] and the precession ages of *Hilgen* [1991a] are minor (a few kiloyears) except for S10 (291 and 331 ka) and S12 (464 and 481 ka). Subsequently, *Lourens et al.* [1996a] showed that alternating thick/thin sapropels reflect the influence of obliquity, whereby thick sapropels correspond to obliquity maxima and thin sapropels to obliquity minima. They also showed that the time lag for the climate response to obliquity approximates that of the precession signal, which suggests that the influence of

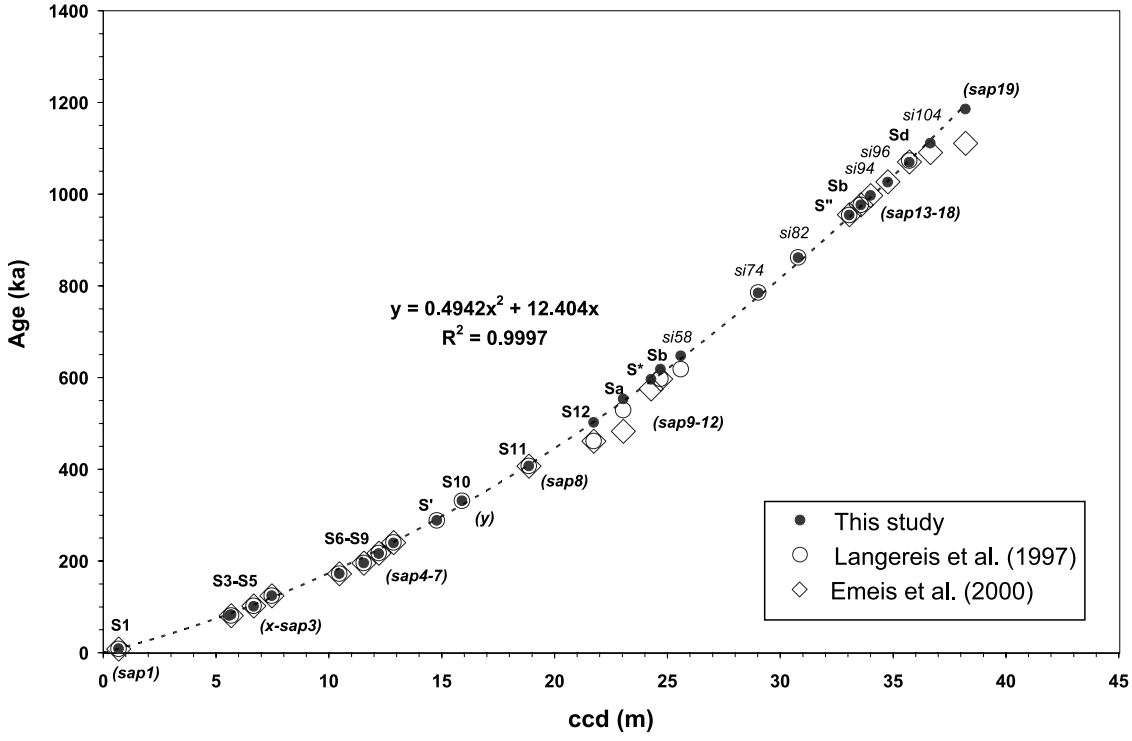

Figure 3. Depth-age plot for ODP Site 964. Indicated are the adopted age models by *Langereis et al.* [1997] (open circles), *Emeis et al.* [2000] (open boxes), and this study (filled circles). Ages and depths are tabulated in Table 4. Indicated are the sapropel codes after, amongst others, *Langereis et al.* [1997] and *Emeis et al.* [2000].

obliquity on sapropel formation in the Mediterranean does not proceed indirectly via glacial cycles but more directly through (summer) insolation. Because the effect of obliquity on insolation decreases markedly at latitudes lower than 60°, they applied the 65°N summer insolation as target curve and included a time lag of 3 kyr (on the basis of the age difference between the radiocarbon dated midpoint of S1 at 8.5 ka and the insolation maximum at 11.5 ka) between the midpoints of each individual sapropel and their correlative insolation maximum. This assumption and the use of the La90 [*Laskar*, 1990; *Laskar et al.*, 1993] 65°N summer insolation as target curve, including present-day values for the tidal dissipation by the Sun and Moon and dynamical ellipticity of Earth, resulted in a refined age model for S1–S12 with differences in age of a few kiloyears compared with the age model of *Hilgen* [1991a].

[22] The sapropel chronologies proposed for KC01B and ODP 964 [*Langereis et al.*, 1997; *Emeis et al.*, 2000] follow the method described by *Lourens et al.* [1996a]. In addition to the sapropel midpoints, *Langereis et al.* [1997] used sapropel-related signals (on the basis of rock-magnetic and geochemical properties) for refining the age model of KC01B. The proposed ages for the sapropels (and sapropel-related signals) of KC01B [*Langereis et al.*, 1997] and ODP Site 964 [*Emeis et al.*, 2000] are compared in Table 2. Both sapropel chronologies adopted the ages of *Lourens et al.* [1996a] for S1–S11 (e.g., S3–S11 in KC01B and SAP1, x, and SAP2–SAP8 in ODP Site 964). *Langereis et al.* [1997] initially also adopted the age of *Lourens et al.* [1996a] for the S12, but spectral analysis of the oxygen isotope record of KC01B revealed a much better fit with the theoretical astronomical cycles (although not shown in the work of *Langereis et al.* [1997]) if the maximum in summer insolation at 461 ka is used. This is in agreement with the previous age estimate for this sapropel by *Rossignol-Strick* [1983]. Also, *Emeis et al.* [2000] adopted this younger age of the S12 for the correlative SAP9 of ODP Site 964. However, the Sa in KC01B and the correlative SAP10 of ODP Site 964 were assigned significantly different tuned ages of 529 and 483 ka, respectively. (The age of 483 ka for sapropel 10 of ODP Site 964 in the work of *Emeis et al.* [2000] appeared to be wrong, while (although not explicitly mentioned) sapropel 10 has been correlated to Sa by *Rossignol-Strick et al.* [1998]). The tuned ages of KC01B and ODP Site 964 are consistent again for sapropels S*/SAP11, Sb/SAP12, S″/SAP13, Sc/SAP14, and Sd/SAP17 and arrive at 575, 597, 955, 977, and 1070 ka, respectively (Table 2). Also, the ages (997 and 1027 ka) of the sapropel-related signals at 33.42 (si94) and 34.10 (si96) mpd in KC01B and the correlatives SAP15 and SAP16 in ODP Site 964 are consistent. The tuned age of the sapropel-related signals at 36.25 mpd in KC01B (1111 ka), however, is 20 kyr older than the tuned age of the correlative SAP18 of ODP Site 964.

[23] The depth-age relationship for ODP Site 964, according to the age models of *Langereis et al.* [1997] and *Emeis et al.* [2000], are shown in Figure 3. This figure clearly reflects a significant change in the depth-age rela-

tionship between S11/SAP8 and S12/SAP9. In addition, major changes in sedimentation rates occur between SAP10 and SAP11 and between SAP17 and SAP18 according to the age model of *Emeis et al.* [2000]. Here I propose an alternative age model based on a more uniform change in the sedimentation rate with time. Starting from this assumption, Sa/SAP10, S*/SAP11, and Sb/SAP12 are tuned one precession cycle older and S12/SAP9 two precession cycles older than proposed by *Langereis et al.* [1997] (Table 2). Moreover, I have adopted the tuned age of *Langereis et al.* [1997] for the sapropel-related signals in KC01B that correlate with SAP18 of ODP Site 964 and retuned SAP19 three precession cycles older than previously proposed by *Emeis et al.* [2000]. The resulting depth-age relationship for ODP Site 964 is accurately described by a second-order polynomial, indicating a gradual decrease in sedimentation rate with age that can be explained by the effect of increased compaction with depth.

[24] According the new timescale, S*/SAP11 and Sb/SAP12 correlate with a low- and high-amplitude summer insolation maximum, respectively, which is in good agreement with the late Pleistocene phase relation as proposed by *Lourens et al.* [1996a]. This is in contrast with the proposed tuning of *Langereis et al.* [1997] and *Emeis et al.* [2000] in which these sapropels are correlated one precession cycle younger and hence results in a less good fit with the insolation pattern. The re-tuning has the important consequence, however, that Sa/SAP10 correlates with a very low amplitude 65°N summer insolation maximum at 553 ka (Figure 4), which cannot be simply explained in terms of the late Pleistocene astronomical phase relations (see also section 4.2). However, Sa/SAP10 correlates with a higher-amplitude precession minimum than in previous tuning efforts by applying the new age model (not shown). Another unexplained question is why the preceding high-amplitude 65°N summer insolation maximum at 575 ka is not reflected by a (distinct) sapropel, while the *Globigerinoides ruber* oxygen isotope record of KC01B is characterized by significantly depleted values (Figure 4). Unpublished Ba/Al and $\delta^{18}O_{G.ruber}$ data from the time equivalent interval at ODP Site 967 reveal, however, that the correlative shift in $\delta^{18}O_{G.ruber}$ is accompanied by an increase in the Ba/Al ratio. These characteristics are similar to those of the S′ level, where the correlative high-amplitude 65°N summer insolation maximum is not reflected by a sapropel either, nor by a drop in the color reflectance record, but by an increase in Ba/Al values. Whether these characteristics are caused by a distinctive response of the climate system to the astronomical forcing or result from diagenetic processes is at present unclear.

[25] A plot of the color reflectance records of KC01, KC01B, and ODP Site 964 against the new age model is shown in Figures 5a and 5b. For this purpose I have corrected the depth scale of KC01 and KC01B to that of ODP Site 964 and have assigned the new astronomical ages to the corrected sapropel midpoints. Moreover, new astronomical ages of three ghost sapropels, si58, si74, and si82, are included for the nonlinear change in sediment accumulation rates between Sb/SAP12 and S″/SAP13. Linear interpolation between these sapropels would result in ages that are approximately 10 kyr older for sediments halfway the interpolated interval. The newly tuned age of si58 is approximately 30 kyr older (equal to 2 short precession cycles) than previously proposed by *Langereis et al.* [1997], whereas the ages of si74 and si82 remained unchanged. All three-calibration points nicely fit the second-order polynomial (Figure 3).

4.2. Oxygen Isotope Chronology

[26] A comparison between the oxygen isotope chronologies for KC01B of *Rossignol-Strick et al.* [1998] and this study and a stacked benthic oxygen isotope record derived from three ODP Sites at Ceara Rise (data from *Bickert et al.* [1997]) is shown in Figure 6. The timescale of *Rossignol-Strick et al.* [1998] was based on tuning the $\delta^{18}O_{G.ruber}$ to the ice volume model of *Imbrie and Imbrie* [1980]. This timescale has subsequently been used to compare the resultant sapropels ages of KC01B with the monsoon index developed by *Rossignol-Strick* [1983]. Both target curves were based on the Ber78 [*Bretagnon*, 1974; *Berger*, 1978] astronomical solution. The pattern in the monsoon index differs slightly from the 65°N summer insolation target curve used by *Langereis et al.* [1997] because of a smaller contribution of obliquity. Notwithstanding this difference and the application of the Ber78 solution in the work of *Rossignol-Strick et al.* [1998] and the $La90_{(1,1)}$ solution in the work of *Langereis et al.* [1997], it is evident that both studies correlate the sapropels to the same precession/insolation peaks. There is, however, one marked difference between both chronologies. *Rossignol-Strick et al.* [1998] did not recognize ghost-sapropel S*, and according to their chronology this level corresponds with a negative value in the monsoon index. This implies that either the geochemical and magnetic signals are not indicative for a ghost sapropel at this level or that the isotope chronology has been miscorrelated. However, the interpretation of *Langereis et al.* [1997] is most likely correct because S* (si54) correlates with SAP11 of ODP Site 964.

[27] The new timescale of KC01B has important consequences for the correlation of the $\delta^{18}O_{G.ruber}$ record to the open ocean marine isotopic stages (MISs) 11–19 (Figure 6). In the first place, the oxygen isotope depletions associated with S12, Sa, S*, and Sb correlate respectively with MISs 13, 14, 15.3, and 15.5 and not with MISs 12.3, 13.3, 15.2, and 15.3, as proposed by *Rossignol-Strick et al.* [1998]. Evidence that the new isotope chronology of the Ionian Sea $\delta^{18}O_{G.ruber}$ record for these stages is correct comes from time slice measurements of mean sea surface temperature (SST) estimates based on $U^{K'}_{37}$ indices ($SST_{alkenones}$) (data are from K.-C Emeis in his review comments of *Emeis et al.* [1998] and *Doose* [1999]). The mean $SST_{alkenones}$ values of S12 and SAP9 arrive at ~19.5 and ~20.2°C, respectively, which strengthen the interpretation that this sapropel correlates with MIS 13 and not with MIS 12.3. In addition, the $SST_{alkenones}$ estimates of Sa of ~14.2°C and SAP10 of ~14.5°C strongly support the new age model, which place this sapropel within glacial MIS 14. This interpretation is sustained by palynological evidence that indicate a cold and dry Mediterranean climate [*Rossignol-Strick et al.*, 1998; *Rossignol-Strick and Paterne*, 1999] during this time inter-

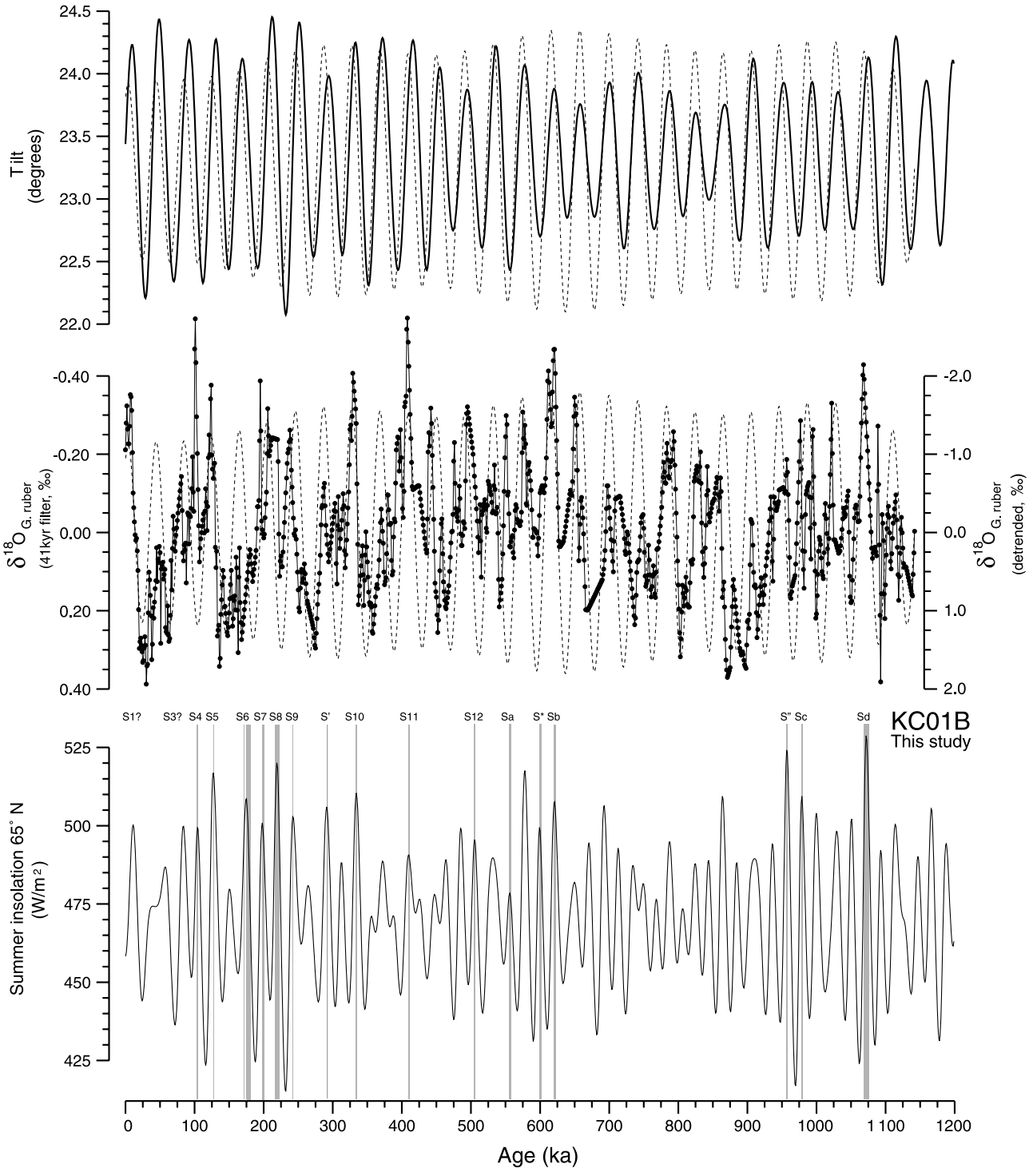

Figure 4. Comparison between the detrended oxygen isotope chronology for KC01B as proposed by this study, the filtered $\delta^{18}O$ 41 kyr component (Gaussian filtering at frequency 0.024289 ± 0.002000), and the $La90_{(1,1)}$ astronomical cycle of obliquity. A summary of the sapropel chronology as presented in this study in relation to the 3 kyr lagged $La90_{(1,1)}$ 65°N summer insolation target curve [*Lourens et al.*, 1996a] is shown in the bottom panel.

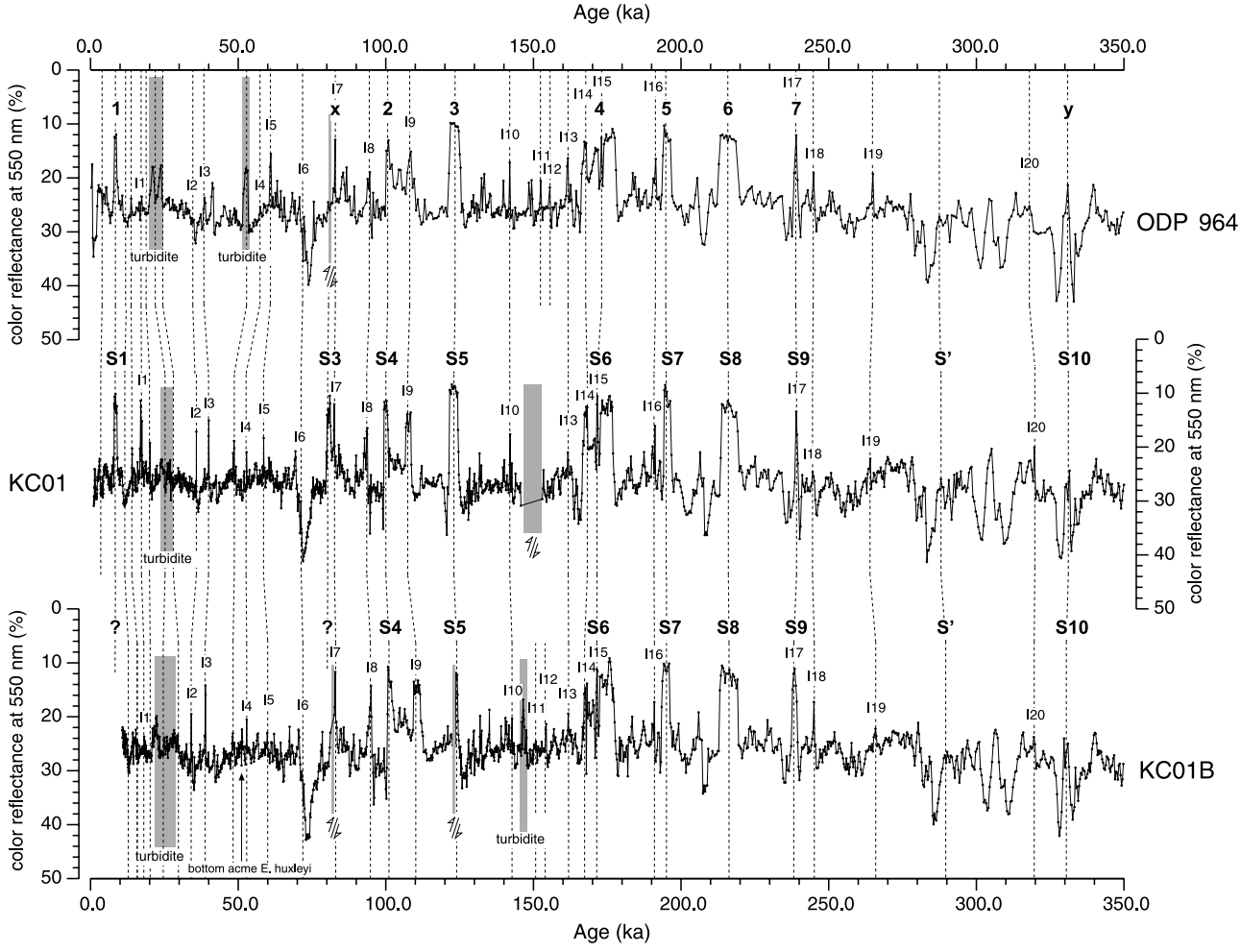

Figure 5a. Color reflectance at 550 nm (%) for cores KC01B, KC01, and ODP Site 964 against age in thousands of years before present. Sapropels for KC01 and KC01B are coded after, amongst others, *Langereis et al.* [1997], whereas the nomenclature for ODP Site 964 is after *Emeis et al.* [1996]. The numbers I1-I33 indicate Tephra layers. Plotted is the time interval between 0 and 350 ka.

val. *Rossignol-Strick et al.* [1998] interpreted Sa/SAP10, however, as an exceptional monsoon event, which they correlated to an event termed ''Y,'' reflected in the $\delta^{18}O_{G.ruber}$ records from two Indian Ocean cores [*Bassinot et al.*, 1994]. Following the new age model for KC01B, this implies that either the correlation of event Y to MIS 13.3 by *Bassinot et al.* [1994] is not correct or that Sa and Y are not related to one another.

[28] SAP11 (S* in KC01B) reveals a mean $SST_{alkenones}$ value of ~19.2°C, while the $\delta^{18}O_{G.ruber}$ mean value is relatively heavy (+0.4‰) with respect to the light$\delta^{18}O_{G.ruber}$ mean values (−0.8‰) of the preceding Sb/SAP12. Apparently, S*/S11 has been formed under lower SST, higher sea surface salinities (SSS) and/or higher global ice volume conditions than Sb/SAP12. Unfortunately, the presently available $SST_{alkenones}$ estimates of Sb/SAP12 by the different authors gave some conflicting results. The data of Emeis arrive at an average $SST_{alkenones}$ value of 15.8°C for Sb/SAP12, reflecting neither full glacial nor interglacial conditions. Taking a closer look at Figure 6 shows that the base of Sb/SAP12 falls close to the MIS 15/16 transition (termination VII) and that the sapropel is characterized by a short interruption in the $\delta^{18}O_{G.ruber}$ record toward heavier values applying the new age model. This isotope pattern is largely mirrored by the $SST_{alkenones}$ data of Site 964 [*Emeis et al.*, 1998] starting with very low SST conditions (~12°C) just below the base of the sapropel followed by an increase toward ~16°C at the base of the sapropel, which drops then to ~14°C in the middle of the sapropel and finally increase again to ~17°C at the top of the sapropel. The $SST_{alkenones}$ has also been measured for Sb of KC01B [*Doose*, 1999]. These data reveal a similar pattern, but the $SST_{alkenones}$ estimates are significantly higher, ~19.8°C for the base and ~18.5°C for the top of Sb than those given by *Emeis et al.* [1998] for SAP12 of ODP Site 964. Thus these data reflect full interglacial values, which are in accordance with the inferred climate conditions during MIS 15.5. The interruption within Sb of KC01B is also recorded by the data of *Doose* [1999], but this drop in SST is also much more extreme (~10.8°C) than that found by *Emeis et al.* [1998].

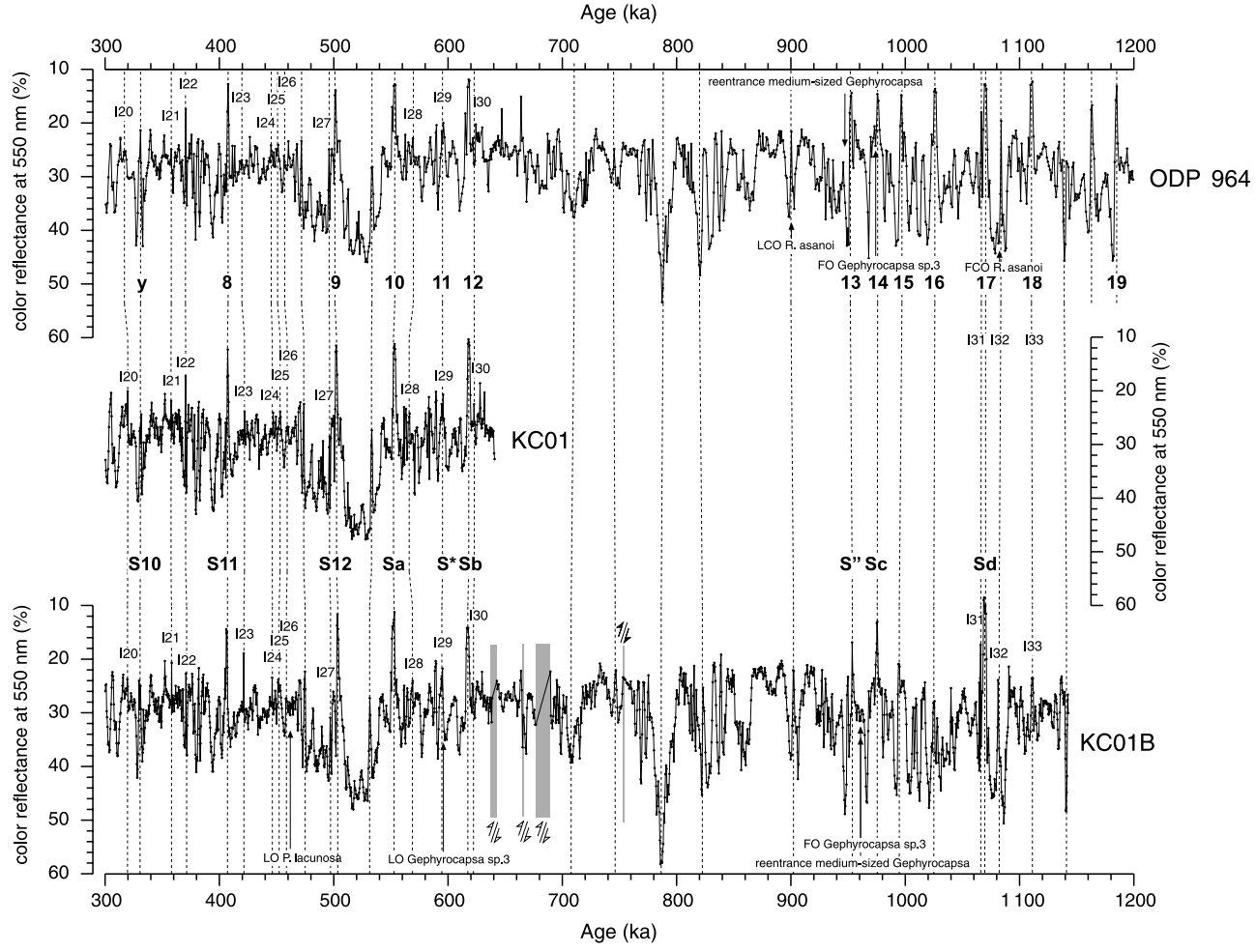

Figure 5b. Color reflectance at 550 nm (%) for cores KC01B, KC01, and ODP Site 964 against age in thousands of years before present. Sapropels for KC01 and KC01B are coded after, amongst others, *Langereis et al.* [1997], whereas the nomenclature for ODP Site 964 is after *Emeis et al.* [1996]. The numbers I1-I33 indicate Tephra layers in the time interval between 300 and 1200 ka.

Evidently, this interruption may reflect a short cooling event or a thin layer of re-deposited sediments of the underlying MIS 16. This further implies that the $\delta^{18}O_{G.ruber}$ record most likely indicates that S*/SAP11 was deposited at times of enhanced SSS and/or global ice volume relative to the preceding Sb, which fits perfectly with the pattern reflected in the open ocean benthic isotope stacked record within MIS 15 (i.e., enhanced ice volume during MIS 15.3 and S*/SAP11 versus reduced ice volume during MIS 15.5 and Sb/SAP12). This observation is in contrast to the age model proposed by *Rossignol-Strick et al.* [1998], where Sb/SAP12 should correspond with MIS 15.3. According to the latter scenario, it will be very difficult to explain the very low SSTs just below this sapropel in relation to MIS 15.4 because such low SST values seem to have occurred only during full glacial conditions.

[29] The new composite depth profile and age model for KC01B between ~25 and ~28 mpd further indicates that the previously interpreted distinct excursions to low $\delta^{18}O$ values during MIS 17 [*Rossignol-Strick et al.*, 1998] represent the tectonic-controlled repetitions of the shift to low $\delta^{18}O$ values in the underlying 19 (Figures 5a–5b). Most likely, the three less extreme oxygen isotope depletions incorporated by *Rossignol-Strick et al.* [1998] in MIS 16 correspond to MISs 17.1, 17.3, and 18.3 (Figures 5a–5b). The oldest part of MIS 16 has probably not been recorded in KC01B owing to tectonic complications between 25 and 25.5 mpd. However, the most important consequences of the new age model for KC01B are the remarkable patterns of the $\delta^{18}O_{G.ruber}$ record during MISs 12 and 16.

4.3. Light $\delta^{18}O_{G.ruber}$ Peaks During MISs 12 and 16

[30] The $\delta^{18}O_{G.ruber}$ of KC01B does not display extremely heavy values throughout the two extreme glacial stages 12 and 16 as would be expected from the open ocean record (Figure 6). Instead, the trend toward heavy values in $\delta^{18}O_{G.ruber}$ is reversed and interrupted by a shift to depleted values in both glacial stages. These shifts have previously been interpreted to reflect the terminations of MISs 12 and 16 [*Rossignol-Strick et al.*, 1998]. Not surprisingly, mistuning of these shifts to glacial-interglacial transitions in an open ocean benthic isotope record will result in

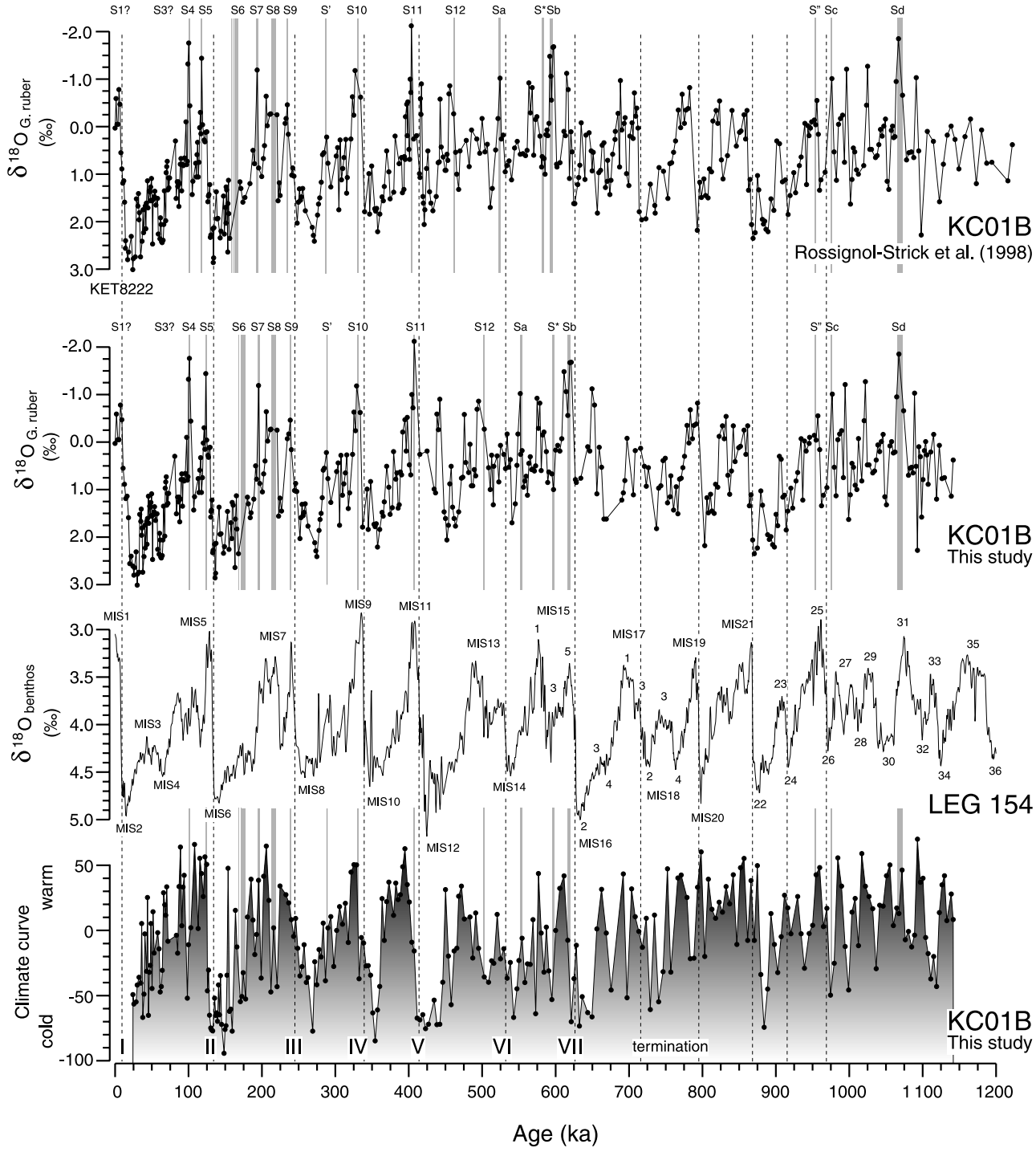

Figure 6. Comparison between the oxygen isotope chronologies for KC01B as proposed by *Rossignol-Strick et al.* [1998] and this study and a stacked benthic oxygen isotope record derived from three ODP sites at Ceara Rise (data from *Bickert et al.* [1997]). At the bottom, the climatic curve as reconstructed by *Sanvoisin et al.* [1993] but re-dated according to the new timescale presented in this study.

significant changes in sedimentation rates (Figure 3). Moreover, mistuning of the sapropels, S12/SAP-Sb/SAP12, remained unobserved because both *Langereis et al.* [1997] and *Emeis et al.* [2000] used the oxygen isotope chronology as constraint on their sapropel chronologies.

[31] Confirmation of the alternative interpretation that the two shifts do not reflect the MISs 11/12 and 15/16 transitions comes from the quantitative planktonic foraminiferal study of KC01B [*Sanvoisin et al.*, 1993]. This study shows that low SST conditions persisted throughout MISs 12 and

16 (Figure 6) according to the new age model, while application of the previous age models result in anomalously cold conditions during the early part of MISs 11 and 15. Consequently, the $\delta^{18}O_{G.ruber}$ excursions to light values during MISs 12 and 16 reflect in fact the interstadial stages 12.3 and 16.3 and not MISs 11 and 15.5, as previously suggested by *Rossignol-Strick et al.* [1998].

[32] To further test the robustness of the new isotope chronology for KC01B, a comparison is made with the isotope chronology of ODP Site 975 (Menorca Rise) in the western Mediterranean [*Pierre et al.*, 1999] (Figure 7). ODP Site 975 has a relatively high sedimentation rate (~8.25 cm/kyr) in comparison with sedimentation rates at ODP Site 964 and cores KC01 and KC01B (~3.75 cm/kyr). The age model of ODP Site 975 is based on isotope stage identification and calibration of the $\delta^{18}O$ record of the planktonic foraminiferal species *Globigerina bulloides* to the orbital derived timescales of *Shackleton et al.* [1990], *Bassinot et al.* [1994], and *Tiedemann et al.* [1994]. All distinct isotopic stages and excursions can be correlated, including the shift in the $\delta^{18}O_{G.ruber}$ record during Sa. Conform the age of *Bassinot et al.* [1994], the tuned age for MIS 13.3 (and MISs 17–18) of *Pierre et al.* [1999] is significantly younger than the new age of KC01B. Application of the new age model for KC01B to ODP Site 975 results in a more uniform change in sedimentation rate with depth than constructed by *Pierre et al.* [1999] (Figure 7). Apparently, *Pierre et al.* [1999] tuned the intervals comprising MISs 9/10, 13–14, 17, and 22, too young by up to 25 kyr.

[33] Assuming that the new timescale is correct leaves us with the important question how to explain the remarkable shifts in the $\delta^{18}O_{G.ruber}$ record during MISs 12 and 16. From unpublished data it appears that also the $\delta^{18}O_{G.ruber}$ record at ODP Site 967 (Eratosthenes Seamount) reveals similar strong depletions during these stages, which may point to (at least) an eastern Mediterranean-wide signal. Spectral analysis results clearly indicate the strong control of the 41 kyr component of Earth's obliquity cycle on these peaks (i.e., maximum tilt values; Figure 4), although the precise timing and amplitude of the minimum $\delta^{18}O$ values are most likely constrained by the influence of the precession cycle. For instance, the peak in the $\delta^{18}O_{G.ruber}$ record during MIS 16 corresponds with the ghost sapropel si58 in KC01B and with a thin sapropel, termed "c," in ODP Site 967 (unpublished data). The fact that the influence of the obliquity cycle is so markedly absent in open ocean records during these two glacial periods suggests that these peaks in the $\delta^{18}O_{G.ruber}$ records of KC01B (and ODP Site 967) are controlled by circum-Mediterranean climate changes. Since the planktonic foraminiferal abundance patterns of KC01B revealed low SSTs, the shifts in $\delta^{18}O$ toward lighter values most likely indicate decreased SSS conditions. Assuming a constant SST of ~12°C and a fixed ice volume during these periods, SSS conditions may have dropped in the order of 12‰. It is emphasized that these extreme salinity drops reflect freshwater-diluted lenses that are floating on top of highly saline subsurface to deep waters at times of full MISs 12 and 16 glacial conditions. *G. ruber* is one of the most euryhaline shallow-dwelling planktonic foraminiferal species [*Hemleben et al.*, 1989]. Its resistance to freshwater disturbances may therefore explain why this species explicitly records the severe drops in $\delta^{18}O$.

[34] Shifts to lighter values in planktonic $\delta^{18}O$ records of the Mediterranean during full-glacial conditions are not restricted to MISs 12 and 16. The most classical examples are those associated with S6 and S8 during the early phase of MISs 6 and 7.4 [e.g., *Cita et al.*, 1977; *Vergnaud-Grazzini et al.*, 1977; *Thunell et al.*, 1983; *Negri et al.*, 1999], respectively, but with the marked difference that the monsoon index of *Rossignol-Strick* [1983] reached relatively large maxima during deposition of these sapropels. Recently, *Emeis et al.* [2003] clearly exposed, however, a second period of much depleted $\delta^{18}O_{G.ruber}$ values in MIS 6 that corresponds with the low-amplitude monsoon index maximum at 150 ka. This strong depletion was not found in KC01B (e.g., Figure 4) but is recorded in three cores east of ~22°E [*Emeis et al.*, 2003]. The geographical distribution of this event may point to a freshwater source coming from the southeastern Mediterranean, suggesting a direct link with a strongly intensified African monsoon [*Emeis et al.*, 2003]. However, this event is not associated with a sapropel, which suggests that only the isotopic signal of in particular *G. ruber* has been amplified owing to an increased density gradient between fresh surface waters and the highly saline intermediate and deep waters at times of the full MIS 6 glacial conditions. This implies that the monsoon circulation was not necessarily exceptional enhanced, which is in much better agreement with the low-amplitude monsoon index maximum at 150 ka. A similar mechanism could also be held responsible for the severe drops in the $\delta^{18}O_{G.ruber}$ record during MISs 12 and 6 and may also shed new light upon the occurrence of the relatively thick Sa/SAP10 and associated severe drop in $\delta^{18}O_{G.ruber}$ values within MIS 14.

4.4. Astronomical Ages of Geomagnetic Reversals and Bioevents

[35] The new timescale results in modifications for the astronomical ages of the geomagnetic events reported by *Langereis et al.* [1997] for KC01B (Table 3). Largest discrepancies are found for the Calabrian Ridge (CR) 2 and 3 short events within the Brunhes, which become ~28 and ~20 kyr older, respectively. The new age estimate for CR3 is concordant with a minimum observed in the global Sint800 composite record derived from worldwide deep-sea records of relative paleointensity [*Guyodo and Valet*, 1999]. Moreover, this event has been identified in a lava flow sequence from La Palma (Canary Islands) and has been dated at 602 ± 12 ka by K/Ar dating using the Cassignol technique [*Quidelleur et al.*, 1999]. Recently, *Singer et al.* [2002] re-dated the La Palma event by using the $^{40}Ar/^{39}Ar$ technique. These authors arrived at a weighted mean age of 580 ± 7.8 ka for this event and argued that this event should correspond with the well-known Big Lost event rather than with a new excursion. One of their arguments referred to the age estimate of CR3 at 573 ka by *Langereis et al.* [1997], who also attributed CR3 to the Big Lost event. *Lanphere* [2000] arrived, however, at a $^{40}Ar/^{39}Ar$ plateau age of 549 ± 6 ka and an isochron age of 542 ± 7.2 ka for

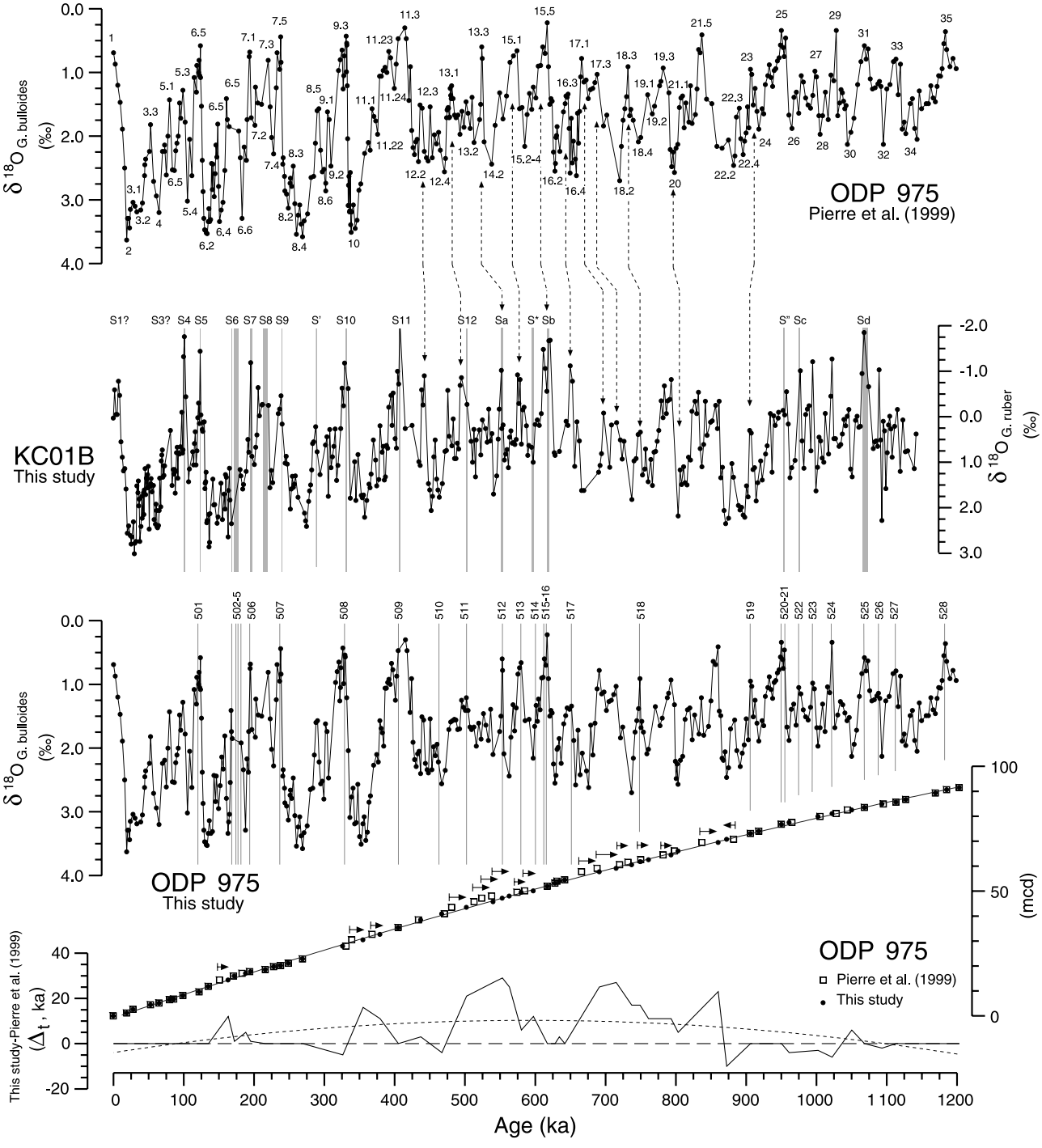

Figure 7. Comparison between the oxygen isotope chronologies for KC01B as proposed by this study and that of ODP Site 975 at Menorca Rise (western Mediterranean) [*Pierre et al.*, 1999]. In the bottom two panels of the figure the ODP Site 975 oxygen isotope chronology has been re-dated in accordance with the age model presented in this study for KC01B and its implications for the age-depth plot of this site has been shown. Arrows indicate the direction and magnitude of change between the ages of the calibration points according to *Pierre et al.* [1999] (open squares) and this study (solid circles). Also indicated are the organic-enriched layers in ODP Site 975 (coding after, amongst others, *Comas et al.* [1996]) and its good correspondence with the sapropel chronology of KC01B.

Table 3. Astronomical Ages (Ma) of Calcareous Nannofossil Datums and Geomagnetic Events[a]

Calcareous Nannofossil Event	OPD Site 964, ccd	This Study	KC01B, mbsf	Age 1	Age 2	This Study
Bottom acme *Emiliania huxleyi* (MNN 21a–21b)	3.75	0.540	4.86			0.520
Bottom *Emiliania huxleyi* (MNN 20–21a)	13.60	0.258	14.95	0.265	0.265	0.264
Bottom acme small *Gephyrocapsa* spp.			14.95	0.265	0.265	0.264
Top *Pseudoemiliania lacunosa* (MNN 19f–20)	20.71	0.468	20.80	0.468	0.440	0.465
Top *Gephyrocapsa* sp.3	23.90	0.583	24.14	0.584	0.577	0.597
Top (common) *Reticulofenestra asanoi*	31.77	0.901				
Reentrance medium *Gephyrocapsa* (>4 micron)	32.87	0.946	32.71	0.944	0.962	0.963
Bottom *Gephyrocapsa* sp.3 (MNN 19e–f)	33.34	0.966	32.71	0.944	0.962	0.963
Bottom (common) *Reticulofenestra asanoi*	36.02	1.082				
		Geomagnetic Event				
CR0			14.83		0.261	0.260
CR1			16.55		0.318	0.319
CR2			22.72		0.515	0.543
CR3			24.05		0.573	0.593
Brunhes/Matuyama	29.76	0.814	29.85	0.780	0.831/0.812*	0.827
Upper Jaramillo			33.52	0.990	1.001	1.001
Lower Jaramillo			35.10	1.070	1.072	1.072

[a]Data of ODP Site 964 have been obtained from *Sprovieri et al.* [1998], P. Maiorano et al. (personal communication, 2003), and *Richter et al.* [1998]. Data of MD69 KC01B have been obtained from *Castradori* [1993] and *Langereis et al.* [1997]. Age 1 refers to the literature ages according to *Castradori* [1993] and *Shackleton et al.* [1990]. Age 2 are the ages obtained by the sapropel and oxygen isotope chronology (asterisks) of *Langereis et al.* [1997].

the Big Lost event, which are significantly younger than argued by *Singer et al.* [2002] but are in close agreement with previous estimates by *Champion et al.* [1996]. The new age of 543 ka for CR2 is also in close correspondence with these estimates of the Big Lost event, suggesting that they may reflect the same excursion. In addition, according to these age estimates, the Big Lost/CR2 event is concordant with a (split) minimum in the global Sint800 composite record, whereas according to the previous age estimate of *Langereis et al.* [1997], this event corresponds with a maximum.

[36] The age of the Brunhes/Matuyama boundary of 827 ka remains significantly older than the generally accepted age of 780 ka [e.g., *Shackleton et al.*, 1990; *Tauxe et al.*, 1996]. Although the Brunhes/Matuyama boundary interval in KC01B is located in a zone where only minor diagenesis was thought to have occurred [*Dekkers et al.*, 1994], *Langereis et al.* [1997] assumed that delayed NRM acquisition has probably caused the reversal to appear older. Owing to the high-resolution correlations between KC01B and ODP Site 964 presented in this study, it can now be shown that the position (and age) of the Brunhes/Matuyama boundary in ODP Site 964 [*Richter et al.*, 1998] is in good correspondence with that of KC01B (Table 3). If delayed NRM acquisition has played a role, this should have altered the paleomagnetic signal at ODP Site 964 as well.

[37] Nine calcareous nannofossil datums have been determined in the KC01B-ODP Site 964 template (Table 3). The new ages for the top of *Pseudoemiliania lacunosa* (0.468–0.465 Ma) and the bottom of *Gephyrocapsa* sp.3 (0.966–0.963 Ma) seem to be the most consistent within this template and differ slightly from previous age estimates by *Castradori* [1993] and *Langereis et al.* [1997].

4.5. Ionian Sea Tephra Chronology

[38] The ages of each tephra layer from KC01, KC01B, and ODP Site 964 are given in Table 4. These ages were used to tentatively identify the most prominent layers in terms of the tephra chronology of *Keller et al.* [1978]. *Keller et al.* [1978] developed a nomenclature for the tephra layers on the basis of their relative position within the faunal zones U-Z (U being the oldest, Z the youngest) as defined by *Ericson et al.* [1961] and imported to the Mediterranean sediment succession by *Ryan* [1972]. All tephra layers were given a numerical value, where for example W-1 is being younger than W-3, etc.

[39] Starting from the top of zone Y, the interpolated astronomical age for I1 of 16.7–17.3 ka is slightly older than the literature age of the Y-1 layer dated at ~14 ka by conventional ^{14}C dating [*Kraml*, 1997]. The Y-1 layer has been identified in *Meteor* cores M25/4-10, 11, and 13, which were taken close to KC01, KC01B, and ODP Site 964 and also revealed an interpolated age estimate based on the sapropel chronology of *Lourens et al.* [1996a] of 16.7–17.6 ka [*Kraml*, 1997]. This estimate is similar to that of I1, and as a consequence, I1 is most likely the equivalent of the Y-1 and therefore related to the Biancavilla-Montalto Ignimbrite of Etna [e.g., *Narcisi and Vezzoli*, 1999].

[40] The Y-3 layer (~23–25 ka) has been found in some cores from the Ionian Sea [*Kraml*, 1997; *Narcisi and Vezzoli*, 1999]. The trachytic composition of Y-3 has been interpreted to be of Campanian origin [*Keller et al.*, 1978; *Paterne et al.*, 1986]. The relative position and thin expression of I2 in KC01, KC01B, and ODP Site 964 suggest that this layer may correspond with Y-3, although its age estimate of 34.1–35.8 ka is significantly older than the literature age (Table 4).

[41] Layer I3 is a very distinct tephra layer and its estimated age of 38.3–40.0 ka is in very good agreement with the $^{40}Ar/^{39}Ar$ age of 39.44 ± 0.12 ka obtained by *Gans et al.* [1999] for the large Campanian Ignimbrite. The Y-5 is currently correlated with this large Campanian Ignimbrite eruption of the Phlegrean Fields [*Thunell et al.*, 1979] and is the most widely dispersed ash in the Ionian Sea [e.g., *Narcisi and Vezzoli*, 1999]. Y-5 has also been identified in cores M25/4-10 to 13 and revealed an interpolated age estimate based on the sapropel chronology of *Lourens et al.*

Table 4. Tephra Chronology of KC01, KC01B, and ODP Site 964

Tephra	KC01B		KC01		ODP 964		Literature					
Ionian	Level,[a] m	Age_{new}, kyr	Level,[a] ccd	Age_{new}, kyr	Level,[a] ccd	Age_{new}, kyr	Name[b]	Origin	Age, kyr	Reference	Age, kyr	Reference
I1	1.275	16.7	2.350	16.9	1.283	17.3	Y-1 (Et-1)	Etna			16.4	*Kraml* [1997]
I2	3.370	34.1	4.505	35.8	2.465	34.7	Y-3 (C-7/8)	Campanian				
I3	3.835	39.1	4.950	40.0	2.706	38.3	Y-5 (C-13)	Campanian	39.44 ± 0.12	*Gans et al.* [1999]	41.1 ± 2.1	*Ton-That et al.* [2001]
I4	4.930	52.6	6.245	52.9	3.972	57.0	Y-7 (C-17)	Ischia			56 ± 4	*Kraml* [1997]
I5	5.430	59.5	6.800	58.7	4.215	60.6	(C-18)	Ischia				
I6	6.240	71.8	7.910	70.8	4.965	71.7	X-2	Campanian				
I7	6.840	82.8	8.930	82.8	5.675	82.8						
I8	7.490	95.1	9.710	93.8	6.324	94.5	X-3 or X-4	Aeolian or Etna			89.5	*Kraml* [1997]
I9	8.205	110.5	10.520	108.2	6.932	108.5	X-6	Campanian				
I10	10.160	142.9	12.410	142.1	8.592	142.0						
I11	10.760	150.8			9.247	152.4						
I12	11.010	154.5			9.439	155.5						
I13	11.410	161.9	13.090	161.6	9.825	161.7						
I14	11.690	167.2	13.420	168.2	10.210	167.8	V-0	Pantelleria			170 ± 21	*Kraml* [1997]
I15	11.930	171.6	13.590	171.6	10.576	174.3	V-2	Roman				
I16	12.720	191.2	14.335	191.2	11.385	191.4						
I17	14.035	238.5	15.485	239.0	12.849	238.3						
I18	14.255	245.0	15.685	244.9	13.099	246.0						
I19	14.975	265.9	16.335	264.1	13.889	269.9	V-4?	Roman				
I20	16.540	319.5	17.845	319.7	15.449	313.4						
I21	17.715	358.6	18.955	357.8	16.950	357.9						
I22	18.125	371.4	19.360	370.4	17.443	370.6	Mt	Central Italy			374 ± 7	*Pyle et al.* [1998]
I23	19.645	421.7	20.900	421.9	19.456	426.7						
I24	20.285	446.6	21.510	446.9	20.014	445.1						
I25	20.425	452.0	21.670	453.5	20.206	451.5						
I26	20.675	461.7	21.840	460.4	20.36	456.6						
I27	21.585	497.0	22.745	497.5	21.552	496.0						
I28	23.285	569.2	24.175	566.4	23.514	569.3						
I29	24.005	596.0	24.885	595.6	24.264	595.3	VdD-3	Roman			596 ± 6	*Karner et al.* [1999]
I30	24.505	622.4	25.500	622.6	24.822	622.8						
I31	34.865	1066.1			35.676	1066.8						
I32	35.240	1082.6			36.080	1085.0						
I33	36.020	1111.8			36.666	1111.5						

[a]Levels in meters refer to the modified piston depths of KC01B and corrected composite depth of ODP 964 as used in this study.
[b]Abbreviations are as follows: Mt, Morphi tephra (NW Greece); VdD, Vallo di Diano (S Italy).

[1996a] of 36.7–40.2 ka [*Kraml*, 1997], which is similar to that of I3. All this suggests that I3 corresponds with Y-5. *Ton-That et al.* [2001] have recently obtained a slightly older $^{40}Ar/^{39}Ar$ age estimate for Y-5. These authors re-interpreted the origin of the C-13 tephra layer (Tyrrhenian Sea), which had been previously related to the Citara formation from the Ischia volcano [*Paterne et al.*, 1986, 1988], in favor of the Campanian Ignimbrite eruption. This renewed interpretation was based on 51 $^{40}Ar/^{39}Ar$ laser-heating analyses of sanidine crystals recovered from a piston core and chemical analyses of glass shards from the C-13 layer. Twenty-four of the radiometric analyses defined an isochron of 41.21 ± 2.1 ka, which is slightly older but still in agreement with the age estimate of *Gans et al.* [1999] at the 95% confidence level. Nevertheless, an unambiguously distinction between the Campanian Ignimbrite and the Citara Tuff based on glass shards chemistry is limited because of the large overlap in their chemical composition [*Ton-That et al.*, 2001].

[42] Layer I4 has an estimated age between 52.6 and 57.0 ka. This layer is too old to correspond with Y-6, which has a K/Ar age of ~45 ka for the associated Green Tuff of Pantelleria Island [*Cornette et al.*, 1983; *Mahood and Hildreth*, 1986; *Civetta et al.*, 1988]. *Paterne et al.* [1986, 1988] have found several peralkalic trachytic layers (C-16–C-18), which they grouped as the Green Tuff Series and attributed them to the activity of the Ischia volcano. The C-16 and C-17 ash layers were related to the Barano products of Ischia, dated by K/Ar at 51 ± 2.2 ka, and the Green Tuff of the Monte Epomeo of Ischia, dated at an average of 55.4 ± 2.2 ka [*Gillot*, 1984]. The C-17 layer has been linked with Y-7, which has been found in several cores from the Ionian Sea [*Kraml*, 1997] and Lake Monticchio [*Allen et al.*, 1999]. In the *Meteor* cores from the Ionian Sea, Y-7 marks the top of an interval characterized by disperse tephra layers, turbidites and high magnetic susceptibility values. $^{40}Ar/^{39}Ar$ dating of the Y-7 revealed an isochron at 56 ± 4 ka, which is in very good correspondence with the sapropel-derived ages of 53.7 and 57.9 ka from M25/4-12 and -13, respectively [*Kraml*, 1997]. Moreover, this age is in perfect agreement with the 56.250 ka of the Y-7 in Lake Monticchio on the basis of varve counting [*Zolitschka and Negendank*, 1996]. The I4 layer in KC01 and KC01B also marks the top of an interval characterized by disperse tephra

layers, thin turbidites, and high magnetic susceptibility values. Hence all of this strongly suggests that I4 is the equivalent of the Y-7 layer, whereas the underlying I5 layer with an estimated age of 58.7–60.6 ka may well correspond with C-18 (Tyrrhenian Sea), which has an estimated age of ~60 ka [*Paterne et al.*, 1986, 1988] and appears to be widespread in the central Mediterranean [*Narcisi and Vezzoli*, 1999].

[43] Layer I6, dated 70.8–71.8 ka, may represent one of the first tephra layers of zone X. A good candidate is the X-2, which is located just above S3 and has an estimated age of ~70 ka. This layer has been attributed to the Campanian volcanic activity, and its southeastern distribution area extends to at least the Bannock Basin [*Vezzoli*, 1991]. I7 (~82.8 ka) marks a distinct ash layer just below the S3. This layer has been previously interpreted as being the X-2 [*Van Santvoort et al.*, 1997], but its occurrence below the S3 instead of above makes this interpretation less feasible. This layer could not be assigned to one of the tephra layers in the scheme of *Keller et al.* [1978]. Layer I8 with an age estimate between 93.8 and 95.1 ka is a very pronounced layer and could be the equivalent of X-3 and/or the X-4, which have ages of ~90 ka [*Narcisi and Vezzoli*, 1999]. X-4 is an alkali basalt and it has been attributed to the activity of Etna [*Keller et al.*, 1978]. This layer, however, has been found in only one *Meteor* core (22M-60). The same holds true for the X-3, which has been linked to the activity of the Aeolian Islands and was found in only one *Vema* core (V10-69). Layer I9 is again a very pronounced layer and has an age estimate of 108.2–110.5 ka. This layer can easily be correlated to X-6, which was found in the nearby *Meteor* cores M25/4-10 to -13 [*Kraml*, 1997]. X-6 has an approximate age of 110 ka [*Narcisi and Vezzoli*, 1999], and its trachytic composition is probably of Campanian origin [*Keller et al.*, 1978].

[44] Layers I10–I13 are all within zone W. The age for I10 of 142.0–142.9 ka is in good agreement with the estimated age of the W-1 [*Narcisi and Vezzoli*, 1999]. The W-1 has been attributed to the Roman volcanic area [*Keller et al.*, 1978].

[45] One thin but well-expressed tephra (I15) is observed within S6 and has been tentatively labeled as the Roman V-2 [*Keller et al.*, 1978]. A thick tephra (I14) has been identified in the top part of the S6, which was not included in the tephra chronological scheme of *Keller et al.* [1978]. On the basis of core M25/4-12, *Scheld* [1995] characterized and added three new tephra layers (W-0, V-0, and V-4) to the nomenclature of *Keller et al.* [1978], of which the V-0 occurs at a similar position relative to the S6 as the I14 in KC01, KC01B, and ODP Site 964. V-0 has been $^{40}Ar/^{39}Ar$ dated by *Kraml* [1997] at 170 ± 21 ka, which is in good agreement with the age estimate of I14 of 167.2–168.2 ka (Table 4). On the basis of its mineral composition and glass shards, V-0 has been attributed to the volcanic activity of the Pantelleria Island [*Scheld*, 1995]. Layer V-4 has been related to the volcanic activity in the Roman Comagmatic Province and revealed an astronomical age of 266.8–268.7 ka [*Scheld*, 1995], which is in close correspondence with that of the I19 (264.1–269.9 ka). W-0 was not identified in the present study.

[46] Of the older tephra layers I20–I33, two layers deserve special attention because these layers may correspond to tephra layers found on land that have been $^{40}Ar/^{39}Ar$ dated. The first layer is the I22, which obtained an astronomical age of 370.4–371.4 ka. I22 is marked by a distinct peak in the color reflectance records and occurs approximately halfway between S10 and S11. The astronomical age of the I22 is in close correspondence with the $^{40}Ar/^{39}Ar$ age of 374 ± 7 ka for the Morphi tephra found at Epirus (NW Greece) [*Pyle et al.*, 1998]. This 2 m thick trachytic volcanic ash deposit has been attributed to one of the largest volcanic eruption of central Italy over the past 400,000 years, although the exact location is still unknown. The second layer is the I29, which occurs within S* and has an astronomical age of 595.3–596.0 ka. This age is almost similar to the $^{40}Ar/^{39}Ar$ age of 596 ± 6 ka for the glass shards of the Vallo di Diano tephra bed number 3 [*Karner et al.*, 1999]. This layer is a potassic trachyte and is distinctive owing to its abundant mineral sphene content (34% of the mafic minerals). $^{40}Ar/^{39}Ar$ dates from a pyroclastic flow from the Monti Sabatini (Roman Province) revealed a single-crystal total fusion age on sanidine of 605 ± 11 ka [*Karner and Renne*, 1998]. This age estimate in combination with the similar chemical composition of the glass shards and common sphene content strongly suggests that Monti Sebatini is the eruptive source of VdD-3.

5. Conclusions

[47] The new sapropel-tuned age model of KC01B-ODP Site 964 results in a revised oxygen isotope chronology for the Ionian Basin (eastern Mediterranean) of the last 1.1 Myr. This new chronology results in two prominent excursions in the planktonic $\delta^{18}O$ record to light values during both extreme glacial marine isotopic stages 12 and 16. These shifts have previously been interpreted to reflect the MISs 11/12 and 15/16 stage boundaries [*Rossignol-Strick et al.*, 1998]. This misidentification is also largely responsible for discrepancies between the new sapropel-based chronology and earlier attempts made by *Langereis et al.* [1997] and *Emeis et al.* [2000]. The revised isotope chronology has large implications for other Mediterranean-based planktonic foraminiferal isotope records, such as those of *Pierre et al.* [1999] for ODP Site 975 (western Mediterranean) and *Kroon et al.* [1998] for ODP Site 967 (eastern Mediterranean). Moreover, it sheds new light upon the hydrological conditions in the Mediterranean during peak glacial conditions.

[48] **Acknowledgments.** I am grateful to Gert de Lange and the participants of cruise MD69, organized within the framework of the European Union scientific program MAST (Marflux and Palaeoflux) for collecting and providing free excess to the KC01 and KC01B cores. Martine Paterne kindly provided the isotope data of KC01B. Cor Langereis, Frits Hilgen, Jan-Willem Zachariasse, Hirokuni Oda, Kay Emeis, and Dick Kroon are greatly acknowledged for their fruitful comments and suggestions. Special thanks go to Luc Beaufort and Thibault de Garidel-Thoron for stimulating discussions and for organizing my pleasant stay at the CNRS-CEREGE (Aix-en-Provence). The NWO-funded PIONIER-project (file 800.76.200) and VIDI-grant (file 864.02.007) financially supported this research.

References

Allen, J. R. M., et al. (1999), Rapid environmental changes in southern Europe during the last glacial period, *Nature*, *400*, 740–743.

Bassinot, F. C., L. D. Labeyrie, E. Vincent, X. Quidelleur, N. J. Shackleton, and Y. Lancelot (1994), The astronomical theory of climate and the age of the Brunhes Matuyama magnetic reversal, *Earth Planet. Sci. Lett.*, *126*, 91–108.

Berger, A. L. (1978), Long-term variations of daily insolation and quaternary climatic changes, *J. Atmos. Sci.*, *35*, 2362–2367.

Berger, A. L., and M. F. Loutre (1990), Insolation values for the climate of the last 10 m.y., *Quat. Sci. Rev.*, *10*, 297–317.

Bickert, T., W. B. Curry, and G. Wefer (1997), Late Pliocene to Holocene (2.6–0 Ma) western equatorial Atlantic deep-water circulation: Inferences from benthic stable isotopes, *Proc. Ocean Drill. Program, Sci. Results*, *154*, 239–253.

Bretagnon, P. (1974), Termes à longues périodes dans le système solaire, *Astron. Astrophys.*, *30*, 141–154.

Castradori, D. (1993), Calcareous nannofossil biostratigraphy and biochronology in eastern Mediterranean deep-sea cores, *Rivista It. Paleontol. Stratigr.*, *99*(1), 107–126.

Champion, D. E., M. A. Lanphere, and S. R. Anderson (1996), Further verification and 40Ar/39Ar dating of the Big Lost Reversed Polarity Subchron from drill core subsurface samples of the Idaho National Engineering Laboratory, Idaho, *Eos Trans. AGU*, *77*(46), Fall Meet. Suppl., F165.

Cita, M. B., C. Vergnaud-Grazzini, C. Robert, H. Chamley, N. Ciaranfi, and S. D'Onofrio (1977), Paleoclimatic record of a long deep-sea core from the eastern Mediterranean, *Quat. Res.*, *8*, 169–174.

Civetta, L., Y. Cornette, P. Y. Gillot, and G. Orsi (1988), The eruptive history of Pantelleria Sicily channel in the last 50 ka, *Bull. Volcanol.*, *50, 47–57.*

Comas, M. C., et al. (1996), *Proceedings of the Ocean Drilling Program*, *Initial Reports*, vol. 161, Ocean Drill. Program, College Station, Tex.

Cornette, Y., G. M. Crisci, P. Y. Gillot, and G. Orsi (1983), Recent volcanic history of Pantelleria: A new interpretation, *J. Volcanol. Geotherm. Res.*, *17*, 361–373.

Dekkers, M. J., C. G. Langereis, S. P. Vriend, P. J. M. Van Santvoort, and G. J. De Lange (1994), Fuzzy c-means cluster analysis of early diagenetic effects on natural remanent magnetisation acquisition in a 1.1 Myr piston core from the central Mediterranean, *Phys. Earth Planet. Inter.*, *85*, 155–171.

Doose, H. (1999), Rekonstruktion hydrographischer Verhältnisse im Californienstrom und im europäischen Mittelmeer zur Bildungszeit organisch kohlenstoffreicher Sedimente, *GEOMAR Rep. 78*, 111 pp., GEOMAR Res. Cent. for Mar. Geosci., Christian Albrechts Univ., Kiel.

Emeis, K.-C., et al. (1996), *Proceedings of the Ocean Drilling. Program*, *Initial Reports*, vol. 160, Ocean Drill. Program, College Station, Tex.

Emeis, K.-C., H.-M. Schulz, U. Struck, T. Sakamoto, H. Doose, H. Erlenkeuser, M. Howell, D. Kroon, and M. Paterne (1998), Stable isotope and temperature records of sapropels from ODP Sites 964 and 967: Constraining the physical environment of sapropel formation in the eastern Mediterranean Sea, *Proc. Ocean Drill. Project*, *Sci. Results*, *160*, 309–331.

Emeis, K.-C., T. Sakamoto, R. Wehausen, and H.-J. Brumsack (2000), The sapropel record of the eastern Mediterranean Sea—Results of Ocean Drilling Program Leg 160, *Palaeogeogr. Palaeoclimatol. Palaeoecol.*, *158*(3–4), 371–395.

Emeis, K.-C., et al. (2003), Eastern Mediterranean surface water temperatures and $\delta^{18}O$ composition during deposition of sapropels in the late Quaternary, *Paleoceanography*, *18*(1), 1005, doi:10.1029/2000PA000617.

Ericson, D. B., M. Ewing, G. Wollin, and B. C. Heezen (1961), Atlantic deep-sea sediment cores, *Geol. Soc. Am. Bull.*, *72*, 193–286.

Gans, P. B., A. T. Calvert, H. Belkin, W. A. Bohrson, B. De Vivo, G. Rolandi, and F. Spera (1999), Eruptive history of the Campanian ignimbrite (s), Italy from $^{40}Ar/^{39}Ar$ dating (abstract), in *Century of the Pacific Rim: The Past As Prologue to the Future*, vol. 31, no. 6, p. 56, Geol. Soc. of Am., Boulder, Colo.

Gillot, P.-Y. (1984), Datations par la méthode du potassium-argon des roches volcaniques récentes (Pleistocene et Holocene): Contribution à l'étude chronostratigraphique et magmatique des provinces volcaniques de Campanie, des îles Eoliennes, de Pantelleria (Italie du Sud) et de la Réunion (Océan Indien), Ph.D. thesis, 249 pp., Paris-Sud, Paris.

Guyodo, Y., and J.-P. Valet (1999), Global changes in intensity of the Earth's magnetic field during the past 800 kyr, *Nature*, *399*, 249–252.

Hemleben, C., M. Spindler, and O. R. Anderson (1989), *Modern Planktonic Foraminifera*, 363 pp., Springer-Verlag, New York.

Hilgen, F. J. (1991a), Astronomical calibration of Gauss to Matuyama sapropels in the Mediterranean and implication for the geomagnetic polarity time scale, *Earth Planet. Sci. Lett.*, *104*, 226–244.

Hilgen, F. J. (1991b), Extension of the astronomically calibrated (polarity) time scale to the Miocene-Pliocene boundary, *Earth Planet. Sci. Lett.*, *107*, 349–368.

Hilgen, F. J., and W. Krijgsman (1999), Cyclostratigraphy and astrochronology of the Tripoli diatomite formation (pre-evaporite Messinian, Sicily, Italy), *Terra Nova*, *11*, 16–22.

Hilgen, F. J., L. J. Lourens, A. Berger, and M. F. Loutre (1993), Evaluation of the astronomically calibrated time scale for the late Pliocene and earliest Pleistocene, *Paleoceanography*, *8*, 549–565.

Hilgen, F. J., W. Krijgsman, C. G. Langereis, L. J. Lourens, A. Santarelli, and W. J. Zachariasse (1995), Extending the astronomical (polarity) time scale into the Miocene, *Earth Planet. Sci. Lett.*, *136*, 495–510.

Hilgen, F. J., W. Krijgsman, I. Raffi, E. Turco, and W. J. Zachariasse (2000), Integrated stratigraphy and astronomical calibration of the Serravallian/Tortonian boundary section at Monte Gibliscemi (Sicily, Italy), *Mar. Micropaleontol.*, *38*, 181–211.

Hilgen, F. J., H. Abdul-Aziz, W. Krijgsman, I. Raffi, and E. Turco (2003), Integrated stratigraphy and astronomical tuning of Serravallian and lower Tortonian at Monte dei Corvi (middle-upper Miocene, northern Italy), *Palaeogeogr. Palaeoclimatol. Palaeoecol.*, *3178*, 1–36, doi:10.1016/S0031-0182(03)00505-4.

Imbrie, J., and J. Z. Imbrie (1980), Modeling the climatic response to orbital variations, *Science*, *207*, 943–953.

Karner, D. B., and P. R. Renne (1998), $^{40}Ar/^{39}Ar$ geochronology of Roman province tephra in Tibet River Valley: Age calibration of middle Pleistocene sea-level changes, *Geol. Soc. Am. Bull.*, *110*(6), 740–747.

Karner, D. B., E. Juvigne, L. Brancaccio, A. Cinque, E. Russo Ermolli, N. Santangelo, S. Bernasconi, and L. Lirer (1999), A potential early middle Pleistocene tephrostratotype for the Mediterranean basin: The Vallo Di Diano, Campania, Italy, *Global Planet. Change*, *21*, 1–15.

Keller, J., W. B. F. Ryan, D. Ninkovich, and R. Altherr (1978), Explosive volcanic activity in the Mediterranean over the past 200,000 yr as recorded in deep-sea sediments, *Geol. Soc. Am. Bull.*, *89*, 591–604.

Kraml, M. (1997), Laser- $^{40}Ar/^{39}Ar$- Datierungen an distalen marinen Tephren des jung-quartären Mediterranean Vulkanismus (Ionisches Meer, METEOR-Fahrt 25/4), Ph.D. thesis, 216 pp., Univ. Freiburg, Freiburg.

Krijgsman, W., F. J. Hilgen, I. Raffi, F. J. Sierro, and D. S. Wilson (1999), Chronology, causes and progression of the Messinian salinity crisis, *Nature*, *400*, 652–655.

Kroon, D., I. Alexander, M. Little, L. J. Lourens, A. Matthewson, A. H. F. Robertson, and T. Sakamoto (1998), Oxygen isotope and sapropel stratigraphy in the eastern Mediterranean during the last 3.2 myr, *Ocean Drill. Program, Sci. Results*, *160*, 181–189.

Langereis, C. G., M. J. Dekkers, G. J. De Lange, M. Paterne, and P. J. M. Van Santvoort (1997), Magnetostratigraphy and astronomical calibration of the last 1.1 Myr from an eastern Mediterranean piston core and dating of short events in the Brunhes, *Geophys. J. Intern.*, *129*, 75–94.

Lanphere, M. A. (2000), Comparison of conventional K-Ar and 40Ar/39Ar dating of young mafic volcanic rocks, *Quat. Res.*, *53*, 294–301.

Laskar, J. (1988), Secular evolution of the solar system over 10 million years, *Astron. Astrophys.*, *198*, 341–362.

Laskar, J. (1990), The chaotic motion of the solar system: A numerical estimate of the size of the chaotic zones, *Icarus*, *88*, 266–291.

Laskar, J., F. Joutel, and F. Boudin (1993), Orbital, precessional, and insolation quantities for the Earth from −20 Myr to +10 Myr, *Astron. Astrophys.*, *270*, 522–533.

Lourens, L. J., F. J. Hilgen, W. J. Zachariasse, A. A. M. van Hoof, A. Antonarakou, and C. Vergnaud-Grazzini (1996a), Evaluation of the plio-Pleistocene astronomical time scale, *Paleoceanography*, *11*, 391–413.

Lourens, L. J., F. J. Hilgen, I. Raffi, and C. Vergnaud-Grazzini (1996b), Early Pleistocene chronology of the Vrica section (Calabria, Italia), *Paleoceanography*, *11*, 797–812.

Lourens, L. J., F. J. Hilgen, and I. Raffi (1998), Base of large Gephyrocapsa and astronomical calibration of early Pleistocene sapropels in ODP sites 967 and 969: Solving the chronology of the Vrica section, *Ocean Drill. Program, Sci. Results*, *160*, 191–197.

Mahood, G. A., and W. Hildreth (1986), Geology of the peralkaline volcano at Pantelleria, Strait of Sicily, *Bull. Volcanol.*, *48*, 143–172.

Narcisi, B., and L. Vezzoli (1999), Quaternary stratigraphy of distal tephra layers in the Mediterranean—An overview, *Global Planet. Change*, *21*, 31–50.

Negri, A., L. Capotondi, and J. Keller (1999), Calcareous nannofossils, planktonic

foraminifera and oxygen isotopes in the late Quaternary sapropels of the Ionian Sea, *Mar. Geol.*, *157*, 89–103.

Paterne, M., F. Guichard, J. Labeyrie, P. Y. Gillot, and J. C. Duplessy (1986), Tyrrhenian sea tephrochronology of the oxygen isotope record for the past 60,000 years, *Mar. Geol.*, *72*, 259–285.

Paterne, M., F. Guichard, and J. Labeyrie (1988), Explosive activity of the south Italian volcanoes during the past 80,000 years as determined by marine tephrochronology, *J. Volcanol. Geotherm. Res.*, *34*, 153–172.

Pierre, C., P. Belanger, J. F. Saliège, M. J. Urrutiaguer, and A. Murat (1999), Paleoceanography of the western Mediterranean during the Pleistocene: Oxygen and carbon isotope records at Site 975, *Proc. Ocean Drill. Program*, *Sci. Results*, *161*, 481–488.

Pyle, M. D., T. H. Van Andel, P. Paschos, and P. Van den Bogaard (1998), An exceptionally thick middle Pleistocene tephra layer from Epirus, Greece, *Quat. Res.*, *49*, 280–286.

Quidelleur, X., P.-Y. Gillot, J. Carlut, and V. Courtillot (1999), Link between excursions and paleointensity inferred from abnormal field directions recorded at La Palma around 600 ka, *Earth Planet. Sci. Lett.*, *168*, 233–242.

Richter, C., A. P. Roberts, J. S. Stoner, L. D. Benning, and C. T. Chi (1998), Magnetostratigraphy of Pliocene-Pleistocene sediments from the eastern Mediterranean Sea, *Proc. Ocean Drill. Program*, *Sci. Results*, *160*, 61–73.

Rossignol-Strick, M. (1983), African monsoons, an immediate climatic response to orbital insolation, *Nature*, *303*, 46–49.

Rossignol-Strick, M. (1985), Mediterranean Quaternary sapropels, an immediate response of the African monsoon to variation of insolation, *Palaeogeogr. Palaeoclimatol. Palaeoecol.*, *49*, 237–263.

Rossignol-Strick, M., and M. Paterne (1999), A synthetic pollen record of the eastern Mediterranean sapropels of the last 1 Ma: Implications for the time-scale and formation of sapropels, *Mar. Geol.*, *153*, 221–237.

Rossignol-Strick, M., M. Paterne, F. Bassinot, K.-C. Emeis, and G. J. De Lange (1998), An unusual mid-Pleistocene monsoon period over Africa and Asia, *Nature*, *392*, 269–272.

Ryan, W. B. F. (1972), Stratigraphy of late Quaternary sediments in the eastern Mediterranean, in *The Mediterranean Sea*, edited by D. J. Stanley, pp. 149–169, Van Nostrand Reinhold, New York.

Sakamoto, T., T. Janecek, and K.-C. Emeis (1998), Continuous sedimentary sequences from the eastern Mediterranean Sea: Composite depth sections, *Proc. Ocean Drill. Program, Sci. Results*, *160*, 37–59.

Sanvoisin, R., S. d'Onofrio, R. Lucchi, D. Violanti, and D. Castradori (1993), 1 Ma paleoclimatic record from the eastern Mediterranean-Marflux project: First results of a micropaleontological and sedimentological investigation of a long piston core from the Calabrian Ridge, *Il Quat.*, *6*(2), 169–188.

Scheld, A. (1995), Tephralagen in METEOR-Kernen des Ionischen Meeres, M.S. thesis, Univ. Freiburg, Freiburg.

Shackleton, N. J., A. Berger, and W. R. Peltier (1990), An alternative astronomical calibration of the lower Pleistocene timescale based on ODP site 677, *Trans. R. Soc. Edinburg*, *81*, 251–261.

Singer, B. S., M. K. Relle, K. A. Hoffman, A. Battle, C. Laj, H. Guillou, and J. C. Carracedo (2002), Ar/Ar ages from transitionally magnetized lavas on La Palma, Canary Islands, and the geomagnetic instability timescale, *J. Geophys. Res.*, *107*(B11), 2307, doi:10.1029/2001JB001613.

Sprovieri, R., E. Di Stefano, M. Howell, T. Sakamoto, A. Di Stefano, and M. Marino (1998), Integrated calcareous plankton biostratigraphy and cyclostratigraphy at Site 964, *Ocean Drill. Program*, *Sci. Results*, *160*, 155–166.

Tauxe, L., T. Herbert, N. J. Shackleton, and Y. S. Kok (1996), Astronomical calibration of the Matuyama Brunhes Boundary: Consequences for magnetic remanence acquisition in marine carbonates and the Asian loess sequences, *Earth Planet. Sci. Lett.*, *140*, 133–146.

Thunell, R., A. Federman, S. Sparks, and D. Williams (1979), The age, origin, and volcanological significance of the Y-5 ash layers in the Mediterranean, *Quat. Res.*, *12*, 241–253.

Thunell, R. C., D. F. Williams, and M. B. Cita (1983), Glacial anoxia in the eastern Mediterranean, *J. Foraminiferal Res.*, *13*, 283–290.

Tiedemann, R., M. Sarnthein, and N. J. Shackleton (1994), Astronomical timescale for the Pliocene Atlantic $\delta^{18}O$ and dust flux records of ODP Site 659, *Paleoceanography*, *9*, 619–638.

Ton-That, T., B. Singer, and M. Paterne (2001), 40Ar/39Ar dating of latest Pleistocene (41 ka) marine tephra in the Mediterranean Sea: Implications for global climate records, *Earth Planet. Sci. Lett.*, *184*(3–4), 645–658.

Van Santvoort, P. J. M., G. J. De Lange, C. G. Langereis, and M. J. Dekkers (1997), Geochemical and paleomagnetic evidence for the occurrence of "missing" sapropels in eastern Mediterranean sediments, *Paleoceanography*, *12*(6), 773–786.

Vergnaud-Grazzini, C., W. B. F. Ryan, and M. B. Cita (1977), Stable isotope fractionation, climatic change and episodic stagnation in the eastern Mediterranean during the late Quaternary, *Mar. Micropaleontol.*, *2*, 353–370.

Vernekar, A. D. (1972), Long-period variations of incoming solar radiation, Am. Meteorol. Soc., Boston, Mass.

Vezzoli, L. (1991), Tephra layers in Bannock Basin eastern Mediterranean, *Mar. Geol.*, *100*, 21–34.

Zolitschka, B., and J. F. W. Negendank (1996), Sedimentology, dating and palaeoclimatic interpretation of a record from Lago Grande di Monticchio, southern Italy, *Quat. Sci. Rev.*, *15*, 101–112.

L. J. Lourens, Faculty of Geosciences, Department of Earth Sciences, Utrecht University, Budapestlaan 4, N-3584 Utrecht, Netherlands. (llourens@geo.uu.nl)